

F. Schlunegger

Controls of surface erosion on the evolution of the Alps: constraints from the stratigraphies of the adjacent foreland basins

Received: 8 June 1998 / Accepted: 30 October 1998

Abstract The combined information about the stratigraphies from the foreland basins surrounding the Swiss Alps, exhumation mechanisms and the structural evolution of the Alpine orogenic wedge allow an evaluation of the controls of erosion rates on large-scale Alpine tectonic evolution. Volumetric data from the Molasse Basin and fining-upward trends in the Gonfolite Lombarda indicate that at ~ 20 Ma, average erosion rates in the Alps decreased by $>50\%$. It appears that at that time, erosion rates decreased more rapidly than crustal uplift rates. As a result, surface uplift occurred. Because of surface uplift, the drainage pattern of the Alpine hinterland evolved from an across-strike to the present-day along-strike orientation. Furthermore, the decrease of average erosion rates at ~ 20 Ma coincides with initiation of a phase of thrusting in the Jura Mountains and the Southern Alpine nappes at ~ 50 km distance from the pre-20-Ma thrust front. Coupled erosion-mechanical models of orogens suggest that although rates of crustal convergence decreased between the Oligocene and the present, the reduction of average erosion rates at ~ 20 Ma was high enough to have significantly influenced initiation of the state of growth of the Swiss Alps at that time.

Key words Wedge mechanics · Erosion and tectonics · Orogenic system

Introduction

The exhumation and the structural evolution of mountain belts are the result of a critical balance between the rates of crustal thickening and surface erosion (Willett et al. 1993; Batt and Braun 1997). The conceptual

framework for relating the structural evolution and the exhumation of orogens to surface erosion is provided by “critical taper wedge” models for noncohesive frictional Coulomb wedges (Davis et al. 1983; Koons 1994), for viscous wedges (Platt 1986), or for plastic wedges (Chapple 1978; Mandl 1988). Despite differences in the assumptions about rheology and yield conditions between these models, they all conclude that orogenic wedges develop a taper toward the undeformed foreland, thereby reaching a critical value of the sum θ_c of their basal and upper slopes (α and β ; Fig. 1; e.g. Davis et al. 1983; DeCelles and Mitra 1995; Meigs and Burbank 1997). Because basal shear resistance (τ) and gravitational body forces (σ_g) significantly control the critical angle θ_c , surface erosion has a great potential to modify the mechanical state of orogenic wedges. Indeed, as discussed by Platt (1986) and DeCelles and Mitra (1995), enhanced rates of erosion at constant rates of crustal thickening lower the taper to subcritical. As a result, the rear of the wedge must shorten and thicken in order to increase θ to a critical value. On the other hand, a decrease of surface erosion rates at constant rates of crustal thickening increases the taper to a supercritical value. Because the slope is too high, extension may occur, or expansion of the

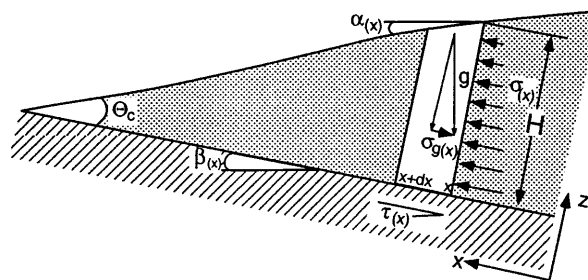


Fig. 1 The body forces (σ_g), shear forces (τ) and compressive push (σ) acting on a moving wedge. g gravitational acceleration; H thickness of wedge at location X ; α surface slope; β basal slope; θ_c critical sum of surface and basal slopes. (Modified after Davis et al. 1983)

F. Schlunegger

Institut für Geowissenschaften Allgemeine und Historische Geologie, Friedrich-Schiller Universität Jena, Burgweg 11, D-07749 Jena, Germany
e-mail: fritz@geo.uni-jena.de

thrust-front towards distal sites is promoted which lowers the average taper to a critical value.

Using the conceptual models outlined herein allows evaluation of the controls of erosion rates on the tectonic evolution of mountain belts provided that detailed information is available concerning (a) the structural evolution of orogens, (b) the thermo-chronological evolution of present-day exposed rocks that can be converted into erosion rates and (c) stratigraphic data from the foreland basins in order to locate the source area and to estimate average supply rates of sediment. If the system is closed, the latter data provide information about temporal variations of average erosion rates that can be compared with the cooling history of the drainage basin. In a laterally open system, which was the case for the North Alpine Foreland Basin (Fig. 2A; Berger 1996), preserved volumes of sediment allow estimates of temporal shifts of supply rates of sediment provided that the significance of sediment bypass on the sediment budget is known.

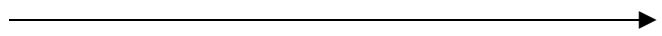
The Oligo-Miocene Alpine system of central Switzerland and northern Italy comprising the Alpine orogenic wedge and the adjacent foreland basins in the north (North Alpine Foreland Basin) and in the south (South Alpine Foreland Basin; Fig. 2) meet most of these requirements through extensive structural, thermo-chronological, chronological, petrological and sedimentological studies as well as finite-element models (Matter 1964; Allen et al. 1985; Gelati et al. 1988; Giger 1991; Sinclair et al. 1991; Bernoulli et al. 1993; Grasemann and Mancktelow 1993; Schmid et al. 1996; Beaumont et al. 1996; Hunziker et al. 1997; Schlunegger et al. 1998; Schlunegger and Willett, in press). Furthermore, this system allows the exploration of the extent of controls of erosion rates on strain partitioning and exhumation, because the shift towards underfilling of the North Alpine Foreland Basin (marine ingression) that occurred at 20 Ma (Keller 1989) coincides with a significant modification in the structural evolution of the Alps from a period of crustal thickening in the central part of the orogen to a phase of frontal accretion in the forelands (Jura Mountains, Southern Alps; Schmid et al. 1996). Schlunegger (1997) hypothesized that the marine ingression at that time was caused by a reduction in average erosion rates. Furthermore, using a two-dimensional coupled erosion-mechanical model for the Alps, Schlunegger and Willett (in press) thought that the hypothesized decrease in erosion rates at ~20 Ma was likely to have changed the structural dynamics of the Alps. These authors thought that the decrease in average erosion rates significantly controlled initiation of deformation of the distal sites of the Alps (Jura Mountains, Southern Alps). Indeed, the decrease in average rates of crustal thickening between the Oligocene and the present (Schmid et al. 1996) would not have initiated a period of orogenic growth towards the forelands if erosion rates would have been constant (e.g. DeCelles and Mitra 1995).

The aim of this paper is to provide further constraints to the hypothesis of Schlunegger and Willett (in press) that erosion influenced the structural evolution of the Swiss Alps between 30 Ma and the present. Stratigraphic data is compiled from the foreland basin in the north to calculate the volume of preserved sediment for different time intervals. These estimates are combined with the knowledge of the significance of axial sediment export/import in an effort to reconstruct temporal changes of average supply rates of sediment. These data are interpreted in terms of variations in Alpine erosion rates. Stratigraphy-based determinations of average erosion rates are compared with the thermo-chronological evolution of present-day exposed rocks that were interpreted by Schlunegger and Willett (in press) in terms of average erosion rates. These estimates are related to the chronology of thrusting in the Alps in order to evaluate the extent of controls of erosion on the structural dynamics of the Alps. The results are evaluated using the coupled erosion-mechanical models of Schlunegger and Willett (in press).

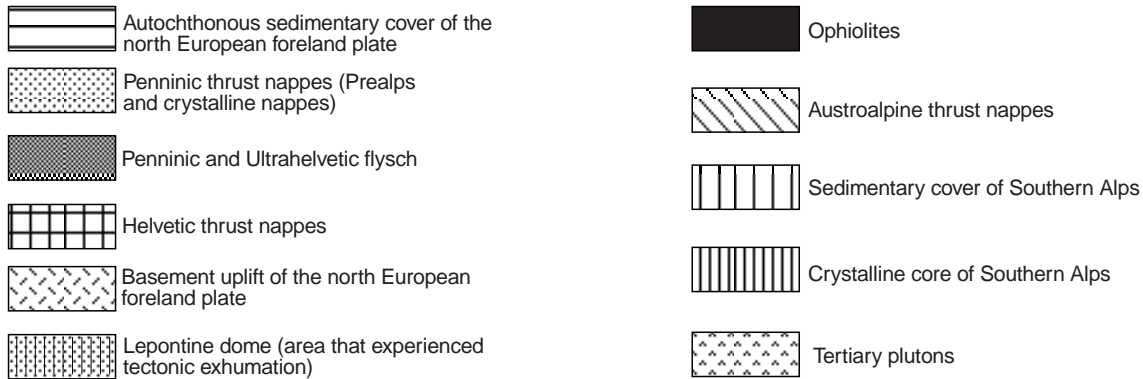
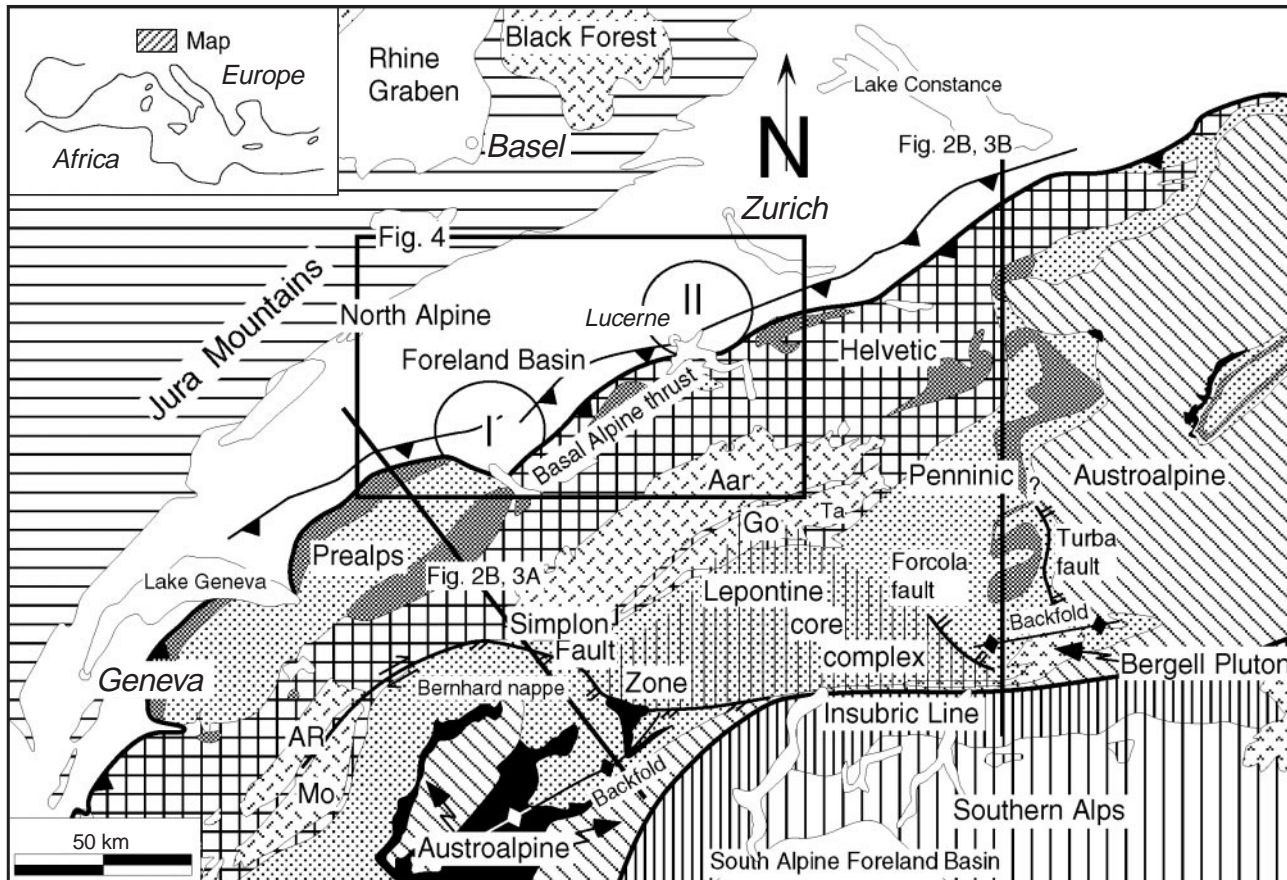
Geological setting

The Alps

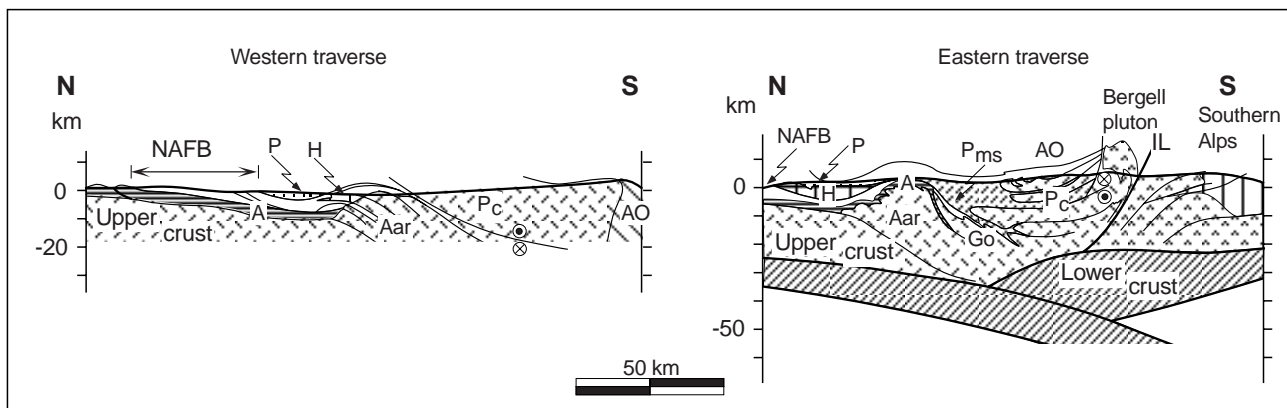
The central Swiss Alps form a doubly vergent orogen that consists of highly metamorphosed crystalline rocks in its core (Lepontine Dome or Lepontine core complex) and low-grade to unmetamorphosed thick-skinned and thin-skinned rocks in their external flanks (Fig. 2A; Schmid et al. 1996). In the north, the present-day Alps comprise the external massifs (e.g. the Aar massif and its autochthonous–parautochthonous cover) and the Helvetic thrust nappes. These units are structurally overlain by the stack of Penninic and Austroalpine nappes. The sedimentary cover of the Penninic thrust nappes that form the Prealps (Fig. 2A) was detached from its crystalline basement prior to 35 Ma (Mosar 1988). The Penninic and Austroalpine nappes are separated from the south-vergent Southern Alps (Fig. 2B; Schönborn 1992) by the east/west-striking Insubric Line that partly accommodated crustal convergence between the European and Apulian plates by


Fig. 2 **A** Map of the Alps and the adjacent foreland basins. The Prealps represent the sedimentary cover of parts of the Penninic crystalline nappes. The Lepontine dome is indicated by a vertical hatched pattern. External massifs: *AR* Aiguilles Rouge; *Mo* Montblanc; *Go* Gotthard; *I* deposits of the Honegg-Napf palaeoriver; *II* deposits of the Rigi-Höhronen palaeoriver. **B** Sections across the western and eastern Swiss Alps (Burkhard 1988; Schmid et al. 1996). *NAFB* North Alpine Foreland Basin; *P* Prealps and flysch; *H* Helvetic thrust nappes; *A* Autochthonous; *P_c* Penninic crystalline nappes; *AO* Austroalpine nappes; *P_{ms}* Penninic metasedimentary nappes (schists and flysch); *IL* Insubric Line; *Go* Gotthard massif

A



B



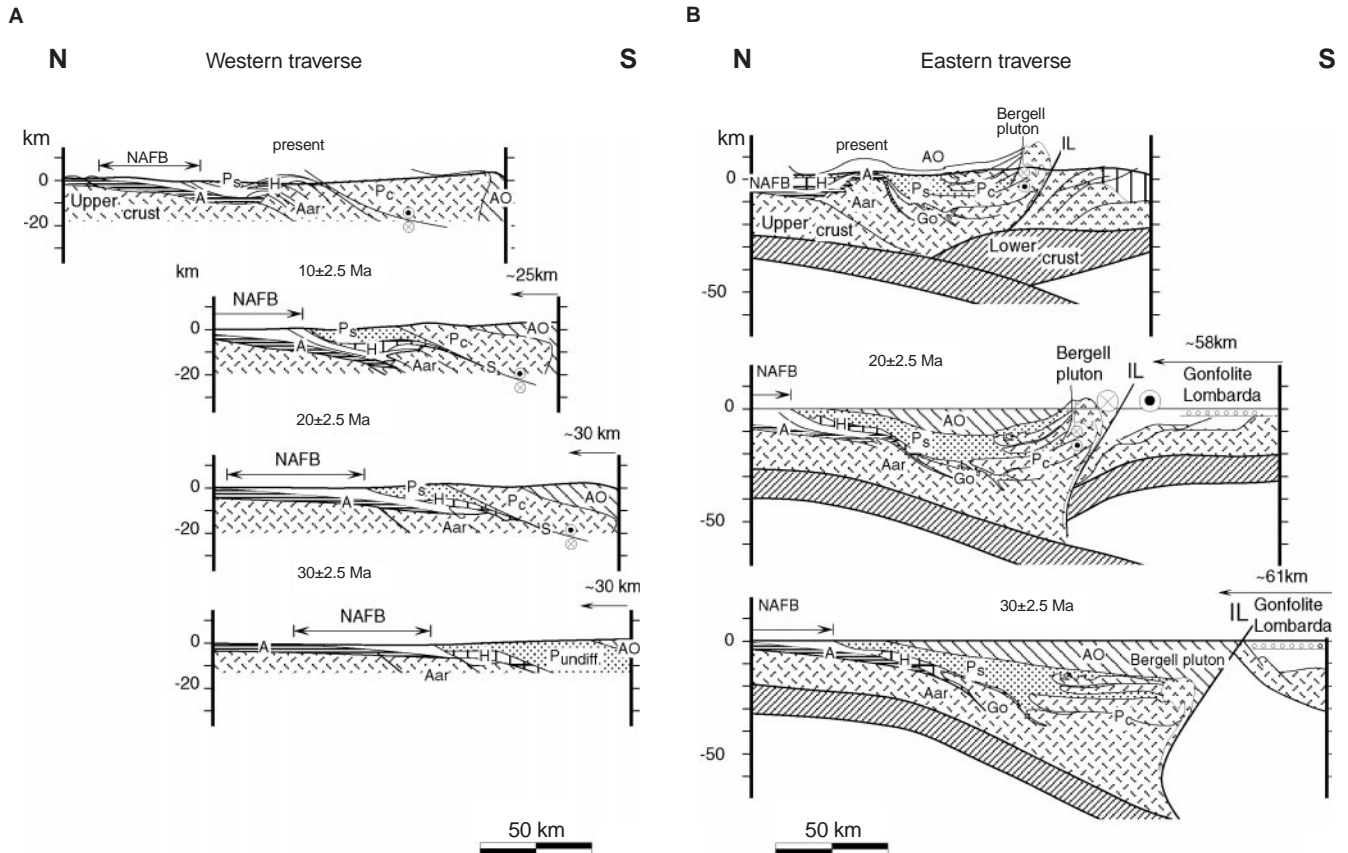


Fig. 3 Sequential palinspastic restoration of the **A** western and **B** eastern Swiss Alps. See Fig. 2B for legend. (Modified after Burkhard 1988, and Schmid et al. 1996)

steep south-directed reverse faulting, coupled with dextral strike-slip faulting (Fig. 3; Schmid et al. 1989, 1996). In the rear of the wedge north of the Insubric Line, the Penninic and Austroalpine nappes were folded due to south-vergent backthrusting along the Insubric Line at some time between ~ 30 and 20 Ma (backfold; Fig. 2A; Steck and Hunziker 1994; Pfiffner and Heitzmann 1997; Schmid et al. 1996). Crustal thickening in the rear of the wedge was associated with east/west-directed crustal extension north of the Insubric Line (Mancktelow 1992; Steck and Hunziker 1994; Schmid et al. 1996) that was accommodated by slip along the Simplon Fault Zone in the west, and the Forcola normal fault in the east (Fig. 2A; Schmid et al. 1996, 1997). According to thermal models of cooling and erosion (Grasemann and Mancktelow 1993; Schlunegger and Willett, in press), maximum rates of extension along the Simplon Fault Zone occurred at approximately 20 Ma.

The external massifs underwent major exhumation during Miocene and Pliocene time. These phases of exhumation coincide with periods of thrusting along steeply dipping faults in the Aar massif that resulted in a vertical throw of >5 km (Pfiffner et al. 1997). These phases of deformation were coeval with thrusting in the

North Alpine Foreland Basin and the Jura Mountains, respectively (Pfiffner et al. 1997). In the Miocene, >45 km of shortening also occurred in the Southern Alps (Lombardic phase of deformation; Schumacher et al. 1997).

The North Alpine Foreland Basin

The peripheral North Alpine Foreland Basin (NAFB), located north of the Alps (Figs. 2A, 4A), is interpreted to have formed as a mechanical response to the tectonic load of the evolving Alps (Homewood et al. 1986; Sinclair et al. 1991; Schlunegger et al. 1997a). The sedimentological development of the NAFB can be described in terms of early deep-water sediments and later shallow-water/continental sediments which have been referred to as Flysch and Molasse in the Alpine literature (Fig. 4; see discussions in Sinclair et al. 1991, Sinclair and Allen 1992). Comparisons between rates of exhumation in the Alps and preserved volume of sediment in the basin suggest that the Molasse represents the late overfilled stage of the evolution of the NAFB (Sinclair and Allen 1992; Sinclair 1997). The Molasse deposits have been traditionally divided into four lithostratigraphic units, for which the conventional German abbreviations are used in this paper (Matter et al. 1980): Lower Marine Molasse (UMM); Lower Freshwater Molasse (USM); Upper Marine Molasse (OMM); and Upper Freshwater Molasse (OSM). They

form two shallowing- and coarsening-upward stratigraphic sequences (Fig. 4B). The oldest sequence comprises the Rupelian UMM, which is overlain by the Chattian and Aquitanian fluvial clastics of the USM. The second sequence, with the transgressive Burdigalian at its base, consists of shallow-marine sandstones (OMM), which interfinger with large fan-delta deposits adjacent to the thrust front (Keller 1989; Mägert 1998; Kempf et al. 1998). This sequence continues up to the Langhian-Serravalian fluvial clastics of the OSM.

Along the southern border of the foreland basin, the Molasse deposits are present in a stack of southward-dipping thrust sheets (Fig. 4A, C, D) referred to as Subalpine Molasse in the Alpine literature. The Plateau Molasse, which represents the more distal part of the basin, is mainly flat lying and dips gently towards the Alpine orogen. Thrusting in the Subalpine Molasse was contemporaneous with sedimentation (Schlunegger et al. 1997a; Kempf et al. 1998).

In the central part of the study area, two transverse drainage systems with sources in the evolving Alps (Honegg-Napf and Rigi-Höhronen palaeorivers; Fig. 2A) drained into a northeastward-flowing axial drainage (Lake Geneva palaeoriver) between 30 and 20 Ma, a shallow peripheral sea (Upper Marine Molasse) between 20 and 16.5 Ma, and a southwestward-oriented axial drainage between 16.5 and 14 Ma (Matter et al. 1980; Berger 1996).

The South Alpine Foreland Basin

The Lower Oligocene to presumably Middle Miocene (Gelati et al. 1988) proximal part of the South Alpine Foreland Basin at the southern border of the Lepontine core complex consists of an approximately 3-km-thick clastic wedge (Bernoulli et al. 1993). Subsidence in this part of the basin is considered as a mechanical response to backthrusting along the Insubric Line and to emplacement of the Southern Alpine nappes (Lombardic phase of deformation; Giger 1991; Schumacher et al. 1996; Schmid et al. 1996; Bertotti et al. 1998). The basin fill starts with the Rupelian Chiasso Formation which comprises an approximately 200-m-thick alternation of silt- and mudstones with sandstone and conglomerate interbeds deposited by turbidity currents (Fig. 5). The presence of large submarine slumps suggests deposition on a slope or base of slope environment (Gunzenhauser 1985). The top of the Chiasso Formation is truncated possibly due to the drastic drop of the eustatic sea level at the Rupelian to Chattian boundary (Bernoulli et al. 1993). Alternatively, this erosional event might have been caused by initial emplacement of the Southern Alpine nappes (Schmid et al. 1996). The overlying Gonfolite Lombarda Group (Fig. 5) consists of two fining- and thinning-upward stratigraphic sequences. The first sequence starts with the ~1500-m-thick Chattian Como Conglomerate which is considered to have been

deposited in a submarine canyon. It ends with an approximately 700-m-thick Aquitanian to Burdigalian alternation of massive sandstones and mudstones that is referred to as the Val Grande Sandstone (Fig. 5). This unit is considered to represent coarsening- and thickening-upward successions of submarine lobes (Bernoulli et al. 1993). The second sequence overlies an unconformity that is interpreted as the result of initiation of the main phase of thrusting in the Southern Alps (Lombardic phase of deformation; Schumacher et al. 1996). This sequence starts with the ~1000-m-thick Burdigalian Lucino Conglomerate which comprises alternating mudstones and sandstones with conglomerate interbeds. This alternation is interpreted to have been formed on a submarine fan. The Lucino Conglomerate is overlain by the Langhian to possibly Serravalian Gurone Sandstone (Fig. 5) composed of alternated mudstones and sandstones. Bernoulli et al. (1993) consider the deposits of the Gurone Sandstone to represent a submarine channel-levee complex.

Supply rates of sediment to the Molasse Basin

Determination of variations in supply rates of sediment to the Molasse Basin is based on isopach maps for the time intervals between 30 and 25 Ma, 25 and 20 Ma (USM) and 20 and 16.5 Ma (OMM). These maps were reconstructed using the thicknesses of sections that were measured in outcrop and in boreholes. The locations of the stratigraphic sections are shown in Fig. 4A, and the data is presented in Fig. 6. The ages of the sections were determined by magnetostratigraphy or by petrographic or seismostratigraphic correlation (Fig. 4A, lines 8307 and 8406; Schlunegger et al. 1997b) with neighbouring temporally calibrated sections. The sections that are located in the folded and thrust part of the Molasse are restored to their palinspastic position using the available information about the timing and amount of shortening (Figs. 4C, 4D). The uncertainties in the restoration of the thrust sheets are discussed in detail by Schlunegger et al. (1993, 1997a) for the western and eastern parts of the basin, respectively. The pinch-out of the Molasse deposits for the different time intervals is taken from palaeogeographic maps by Berger (1996).

The precision of the thicknesses of the strata for the studied time intervals (Fig. 6) strongly depends on the quality of the dating of the analysed sections. The ages of the sediments in the thrust Molasse are reasonably well assessed by magnetostratigraphic calibration (Fig. 6A) or detailed mapping, resulting in error bars of thicknesses of less than 10% (e.g. Schlunegger et al. 1996). The amount of post-sedimentary erosion, however, is not known. Major uncertainties arise for the ages of the strata at Ruppoldsried-1 and Tschugg-1 (Fig. 6B). The ages for these sections were estimated by petrographic correlation with Linden-1 and Thun-1. This speculative approach is justified by the fact that

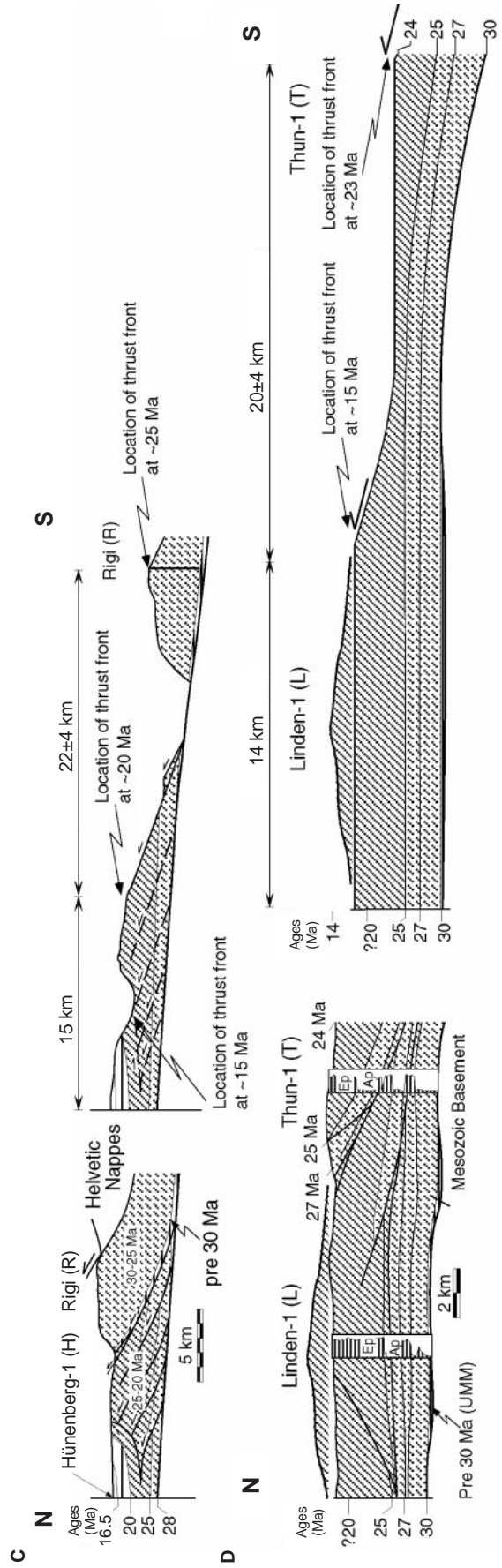
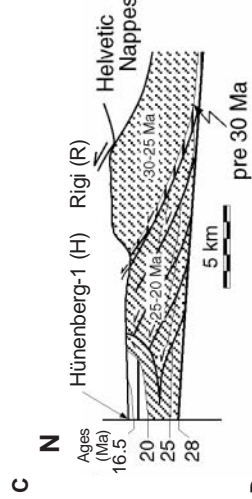
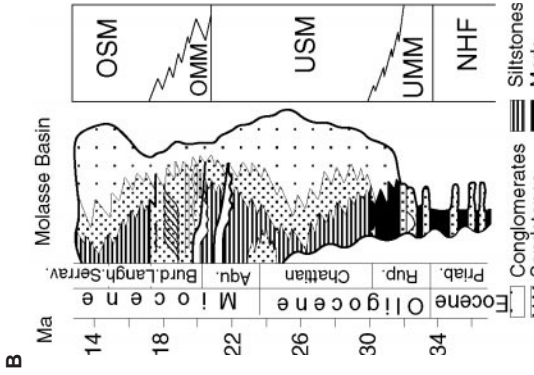
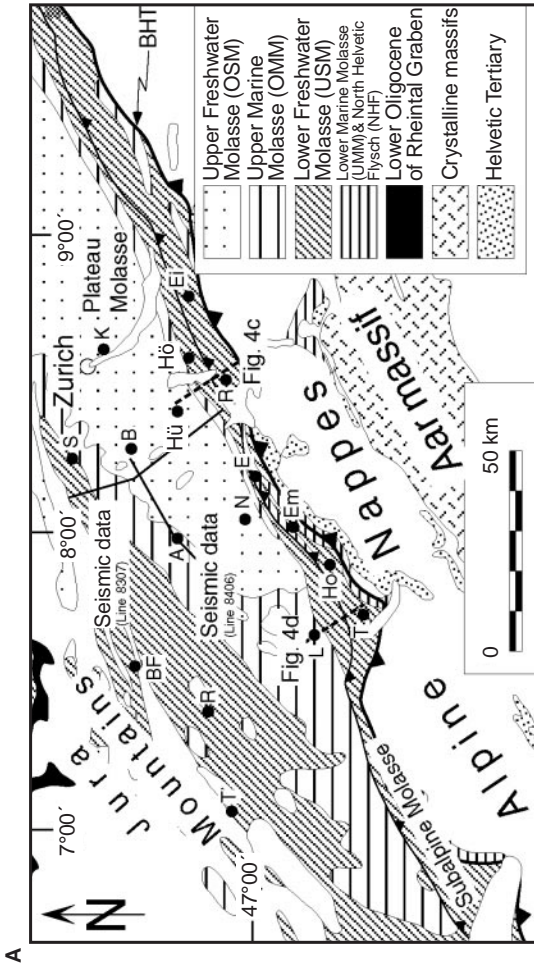


Fig. 4 **A** Map of the Swiss Molasse Basin with location of the stratigraphic sections and the seismic data. *BHT* Basal Helvetic Thrust; The stratigraphic sections are labelled as follows: *T* Thun-1; *L* Linden-1; *Ho* Honegg; *R* Rigi; *Ei* Einsiedeln; *Em* Emme; *Hü* Hünenberg-1; *B* Boswil-1; *S* Schafisheim; *K* Küsnacht-1; *A* Althishofen-1; *E* Entlebuch-1; *R* Ruppoldsried-1; *T* Tschugg-1; *Hö* Höhronen; *BF* Brochene Fluh. **B** Stratigraphic evolution of the Swiss Molasse Basin and chronostratigraphy of the Molasse groups. (Modified after Schlunegger et al. 1996, and Kempf et al. 1998). **C, D** Sections across the eastern and western parts of the Swiss Molasse and palinspastic restoration of the thrust sheets. The calibration of the deposits in the west was achieved through petrographic correlation of heavy mineral suites that were calibrated with magnetostratigraphy (Schlunegger et al. 1996). The section in the west is based on seismic data, and the structural restoration in the east was achieved using surface data that was combined with stratigraphic information from the well Hünenberg-1. The location of the thrust front for different time intervals is taken from Schlunegger et al. (1993, 1997a) for the western and eastern transect, respectively. *Ap* apatite; *Ep* epidote. (Modified after Schlunegger et al. 1993, 1997a)

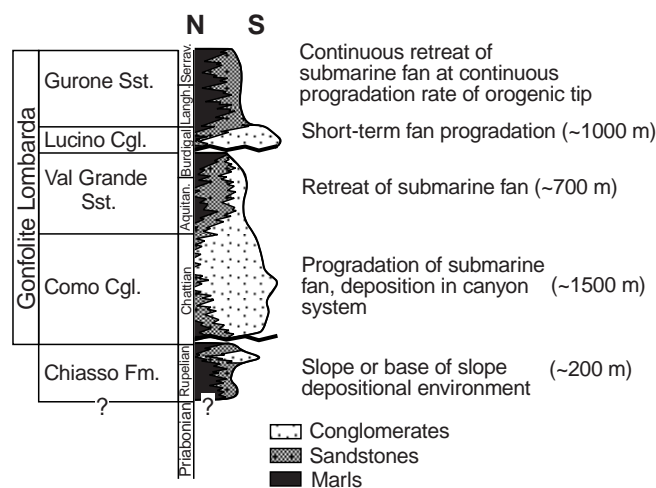


Fig. 5 Large-scale evolution and stratigraphy of the proximal part of the South Alpine Foreland Basin. The compilation is based on sedimentological and stratigraphic data collected by Gelati et al. (1988) and discussed by Bernoulli et al. (1993)

the heavy mineral suites of the sandstones at Thun-1, Linden-1, Ruppoldsried-1 and Tschugg-1 reveal identical trends up-section towards predominance of epidote (Fig. 6B) that appear to be synchronous in the western part of the study area (Schlunegger et al. 1993). The temporal calibration of the strata at Boswil-1 and Hünenberg-1 (Fig. 6C) was achieved by seismostratigraphic correlation with the magnetostratigraphically calibrated Althishofen-1 section (Fig. 4A), resulting in error bars of ± 50 m for the former locations because of the low resolution of the seismic data (Schlunegger et al. 1997b). The ages of the deposits at Entlebuch-1 and Küsnacht-1 were determined from petrographic data collected at these locations (Fig. 6C; Schlanke 1974; Vollmayr and Wendt 1987). These data indicate that in the east, the USM consists of a lower unit (USM I) with a high content of carbonate rock fragments in the sandstone suite, followed by a succession with predomi-

nantly crystalline components in the sandstones (USM II; Schlanke 1974). The transition from USM I to USM II, occurring at ~ 25 Ma according to magneto-polarity chronologies, was considered to be isochronous by Schlunegger et al. (1997a).

Mapping of the isopachs was achieved by hand. Constant thickness gradients were assumed between locations where stratigraphic data are available. The isopach maps and the estimated volume of compacted sediment are presented in Fig. 7. A 10'10-km-wide grid was used for which average thicknesses of compacted sediment were determined. These data were integrated across the study area to calculate the preserved volume of sediment (Fig. 7). Given the uncertainties as outlined herein, error bars of 50% were added for the estimates of the preserved volumes of sediment. However, a careful interpretation of the preserved volume of sediment in terms of sediment supply rates requires correction for porosity that is dependent on lithology and depth. Because the spatial extension of the various lithologies and the maximum burial depths of the analysed locations cannot be determined precisely, corrections for porosities were not calculated. This is justified because the main purpose of this paper is to discuss the relative change of sediment supply rates rather than the absolute magnitudes.

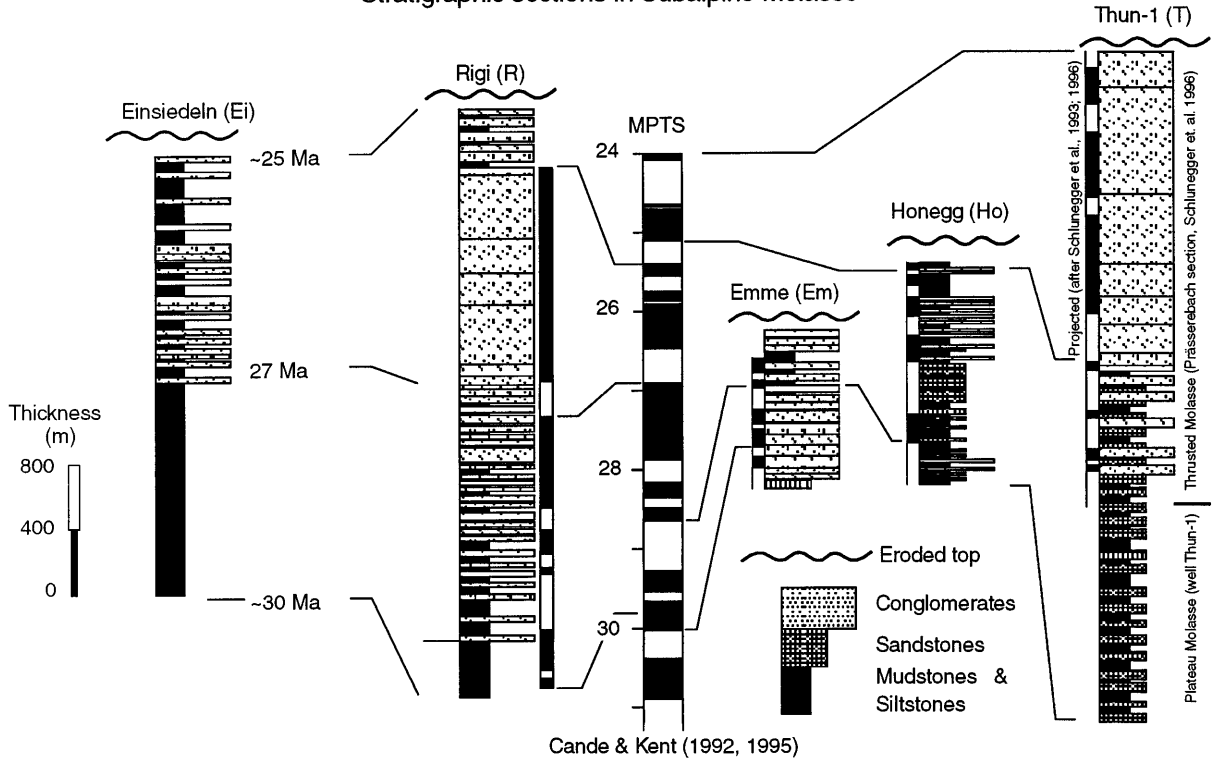
Sediment import and export to a laterally open system, such as the NAFB (e.g. (Füchtbauer 1959, 1964), precludes determinations of absolute values of sediment supply rates to the basin. However, because the purpose of this study is to discuss relative changes of sediment supply rates, and because the time periods of net sediment import and export are known (see below), the use of preserved volume of deposits as proxies for temporal variations in sediment supply rates is justified.

Figure 7A and B shows the location of the deposits of the axial (Lake Geneva) and the transverse palaeorivers (Honegg-Napf, Rigi-Höhronen). The sediments of these rivers were identified based on the occurrence of key heavy minerals in the sandstones (see legend to Fig. 6, 7 for references). Figure 7A and B reveals that between 30 and 25 Ma, and 25 and 20 Ma, a total of $\sim 10,000 \pm 5000$ km³ of sediment was deposited in the

Fig. 6 Stratigraphic data of **A** the thrust Molasse, **B** the Plateau Molasse in the west and **C** in the east. A complete discussion of the temporal calibration of the analysed sections is presented by the following authors: Thun-1 (*T*) (Schlunegger et al. 1993); Honegg (*Ho*) and Brochene Fluh (*BF*) (Schlunegger et al. 1996); Emme (*Em*) (Mägert 1998); Rigi (*R*) and Einsiedeln (*Ei*) (Schlunegger et al. 1997a, c); Höhronen (*Hö*) (Schlunegger et al. 1997a); Hünenberg-1 (*Hü*), Boswil-1 (*B*), Schafisheim (*S*) and Althishofen-1 (*A*) (Schlunegger et al. 1997b); Linden-1 (*L*) (Maurer et al. 1978); Tschugg-1 (*T*) and Ruppoldsried-1 (*R*) (Schlanke et al. 1978). The restoration of the thrust sheets is taken from Fig. 4. The Thun-1 section in **A** and **B** is a composite section of the Plateau Molasse (well Thun-1) and the thrust Molasse (Prässerebach section of Schlunegger et al. (1996))

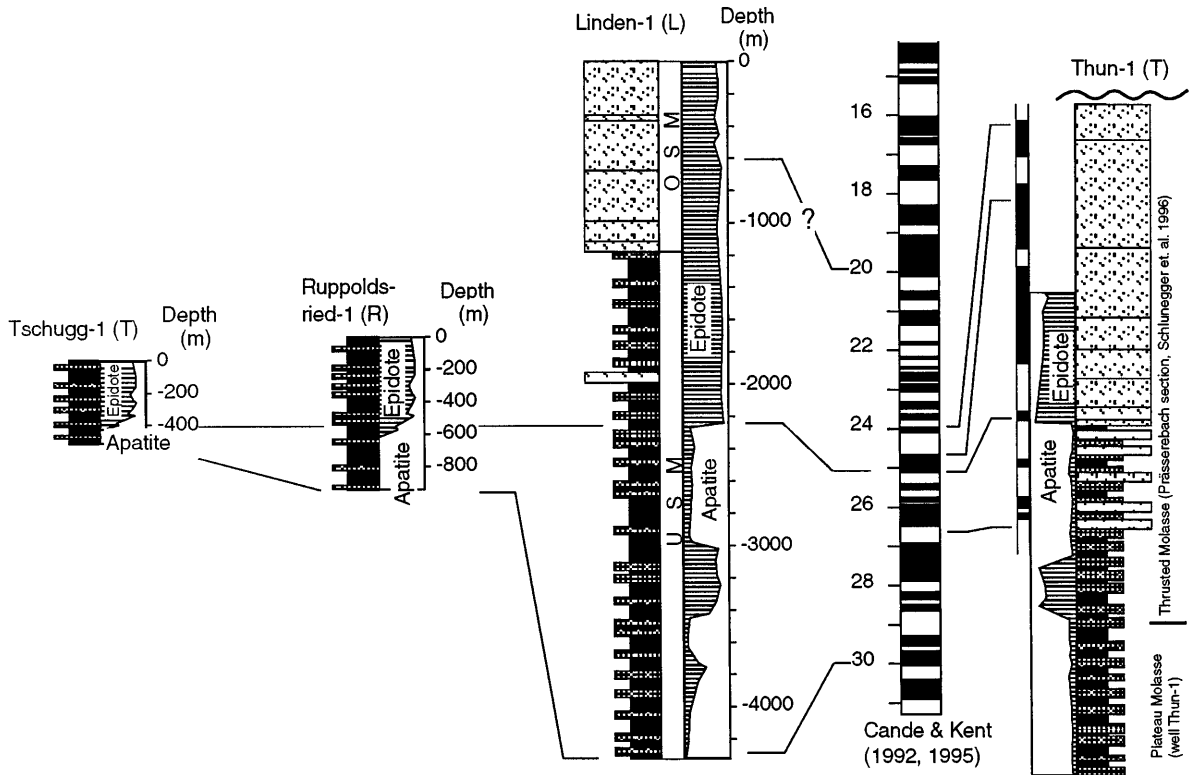
A

Stratigraphic sections in Subalpine Molasse



B

Stratigraphic sections in western part of the Plateau Molasse



C

Stratigraphic sections in eastern part of the Plateau Molasse

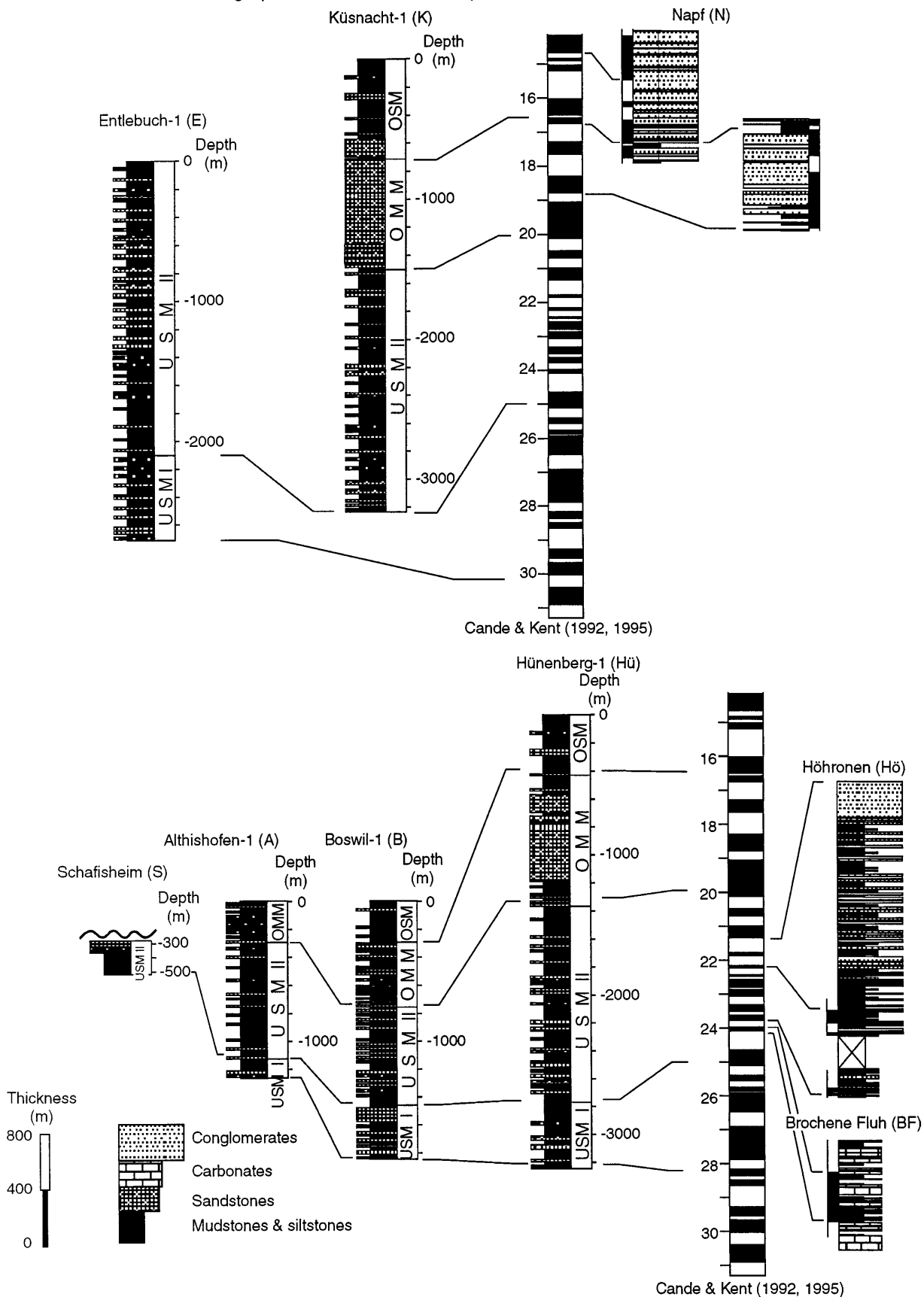
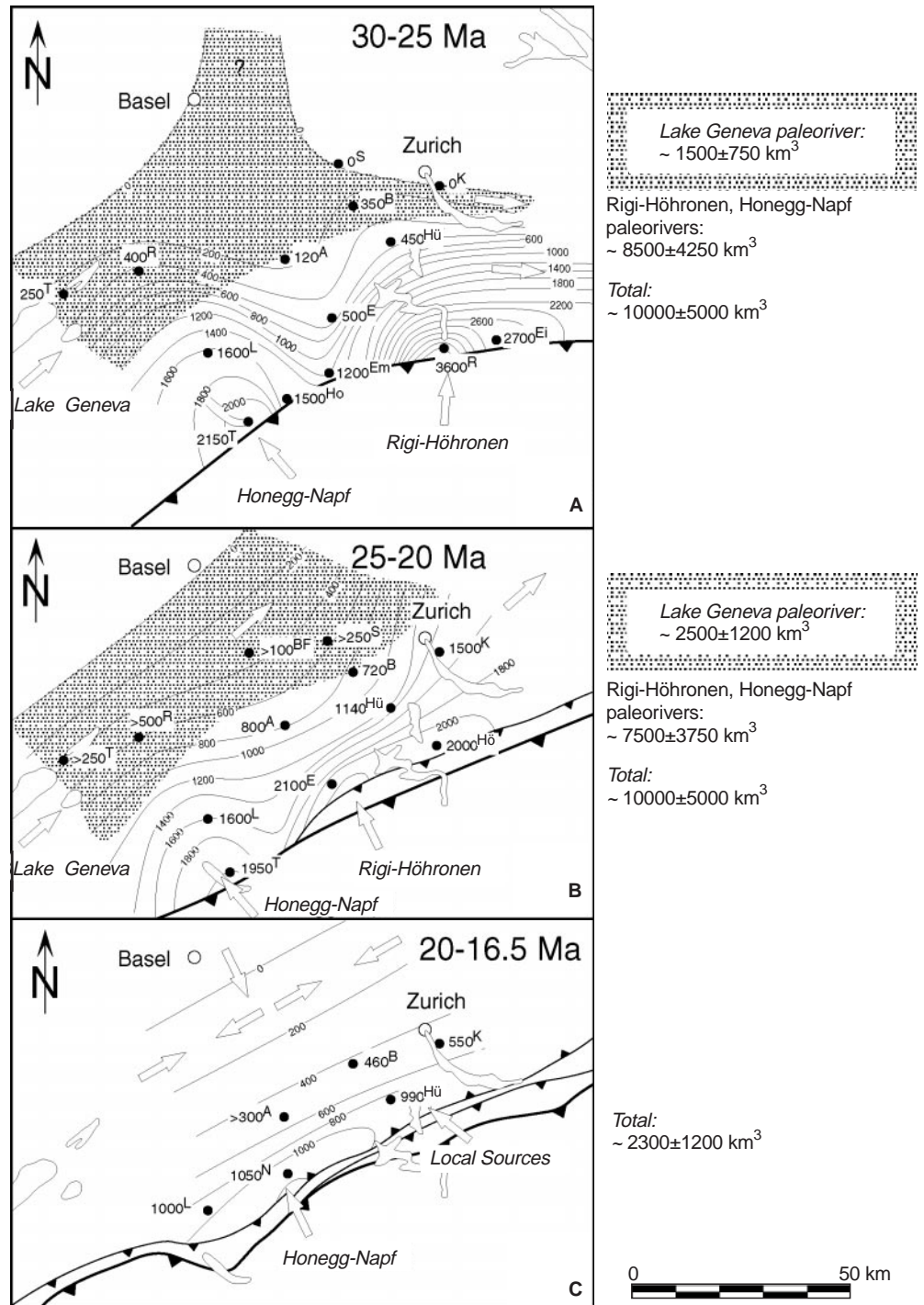


Fig. 7 Isopach maps of the central Swiss Molasse Basin for the time intervals between **A** 30 and 25 Ma, **B** 25 and 20 Ma, and **C** 20 and 16.5 Ma (OMM time). The stratigraphic data as well as the reference list is presented in Fig. 6. The sediment deposited by the axial Lake Geneva palaeoriver between 30 and 20 Ma (sediment import) is indicated by the *grey pattern*. Axial sediment transport during deposition of the OMM (20–16.5 Ma) is indicated by *arrows*. (After Allen et al. 1985)



analysed part of the basin. Of this volume, a minimum of $\sim 7500 \pm 2750 \text{ km}^3$ of sediment was deposited by the transverse Rigi-Höhronen and Honegg-Napf palaeorivers. Because a significant amount of sediment of these palaeorivers bypassed the system in an eastern direction (Fig. 7A, B; Füchtbauer 1959, 1964), the resulting sediment supply rate of $1500 \pm 750 \text{ km}^3/\text{m.y.}$ represents a minimum estimate. During the next time slice, between 20 and 16.5 Ma (deposition of OMM; Kempf et al. 1998), a total of $\sim 2300 \pm 1200 \text{ km}^3$ of sedi-

ment was deposited in the central Swiss Molasse Basin. Because determinations of heavy mineral suites of the OMM sandstones imply a net import of sediment during this time interval (Fig. 7C; Allen et al. 1985), the rate at which sediment was supplied to the study area by the Alpine rivers (Honegg-Napf and local palaeorivers) was a maximum of $650 \pm 325 \text{ km}^3/\text{m.y.}$ This implies at least a $\sim 50\%$ reduction in supply rates of sediment compared with the previous stages of basin evolution.

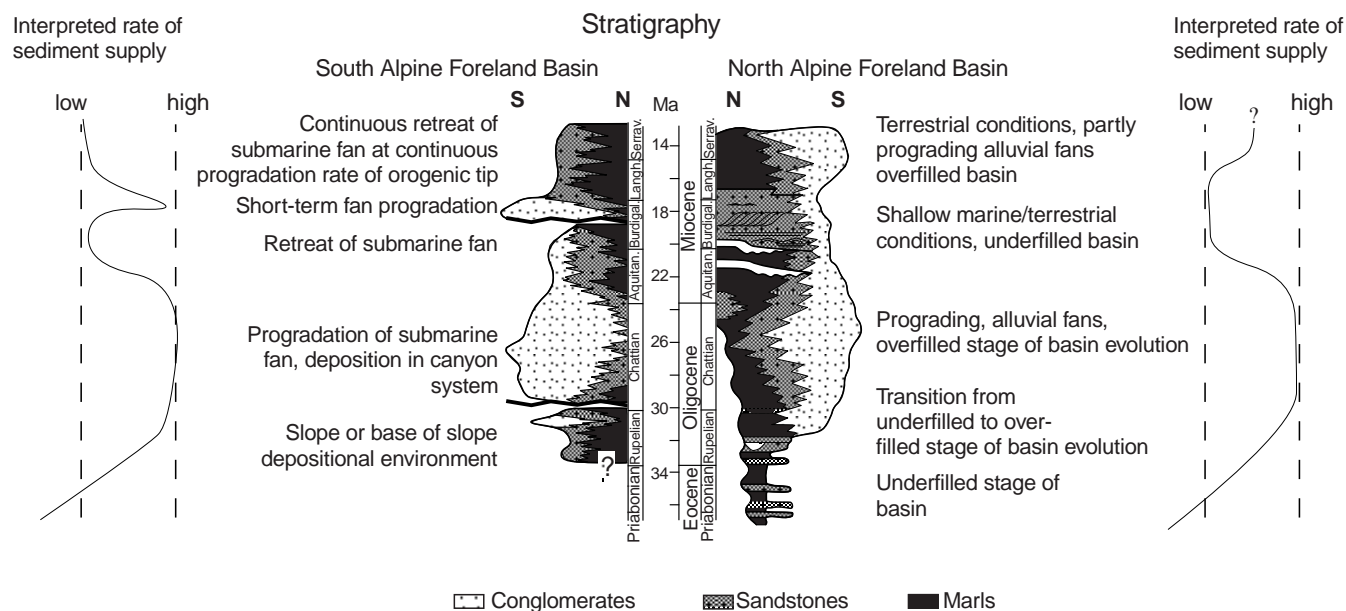
Supply rates of sediment to the South Alpine Foreland Basin

The reconstruction of temporal shifts of supply rates of sediment to the south is based on the combined information about the long-term trend of facies (Fig. 5), sediment accumulation rates and the petrographic evolution. However, as pointed out by Sinclair (1997), a careful estimate of temporal variations of supply rates of sediment requires volumetric data (e.g. see Fig. 7) because of multiple controls on the development of vertical trends of facies. Therefore, the use of the simplified one-dimensional methodology in this paper requires justification:

1. Fan progradation (e.g. Como Conglomerate, Lucino Conglomerate; Fig. 5) might be the result of slowing of advance of the wedge and/or a decrease in the rate of crustal thickening associated with ongoing erosion in the hinterland. The combination of these processes results in uplift of the proximal basin border with respect to the basin axis and a basinward shift of the submarine fans (Flemings and Jordan 1989; Sinclair et al. 1991; Heller and Paola 1992). However, deposition of the Como and Lucino Conglomerates occurred at enhanced rates of sediment accumulation that were considered to result from crustal loading in the rear of the wedge and in the Southern Alps (Schmid et al. 1996). Furthermore, conceptual models of crustal loading and deflection of foreland basins (Turcotte and Schubert 1982; Flemings and Jordan 1989, 1990) indicate that enhanced rates of crustal thickening cause an increase in rates of formation accommodation space (e.g. Bertotti et al. 1998). This implies that deposition of a coarse-grained facies that is associated with enhanced rates of sediment accumulation (e.g. Como Conglomerate, Lucino Conglomerate) reflects enhanced supply rates of sediment.

2. The sedimentological trend of the South Alpine Foreland Basin might be the result of lateral shifts of the submarine fan axis caused by intrinsic and/or extrinsic processes. This interpretation is discarded because the location exhibiting the most proximal sedimentological facies in both the Como and Lucino Conglomerates coincides with the area where the conglomerates reach maximum thicknesses (Gunzenhauser 1985). Furthermore, lateral shifts in the location of the most proximal facies indicative of the fan axis have not been detected despite detailed sedimentological studies (Gunzenhauser 1985). Finally, the sedimentological trends outlined in Fig. 5 comprise time intervals of >5m.y., suggesting extrinsic controls on facies development such as, for example, supply rates of sediment and/or subsidence patterns (Paola et al. 1992). The combined information implies that significant lateral shifts in the fan axis caused by intrinsic and/or extrinsic processes can be discarded.
3. Major volumes of sediment could be ponded within piggyback basins behind the frontal thrusts of the Southern Alpine nappes (e.g. Fig. 3B) before entering the South Alpine Foreland Basin. However, such a scenario results in petrographic trends that are characterized by a succession of clasts derived from structurally lower units, followed by a clast suite that is representative for overlying lithotectonic units (inverse unroofing sequence; Colombo 1994). Similar petrographic trends, however, do not occur in the South Alpine Foreland Basin (Giger 1991). It appears, therefore, that the long-term stratigraphic trend of the South Alpine Foreland Basin,

Fig. 8 Stratigraphy, sedimentology and interpreted evolution of supply rates of sediment to the foreland basins in the north and the south



in combination with information about sediment accumulation rates, is adequate to reconstruct variations of sediment supply rates (see also Heller and Paola 1992).

Figure 8 shows that the stratigraphic evolution of the South Alpine Foreland Basin adjacent to the Lepontine core complex reveals close similarities to the Molasse in the north. In the south, the transition from a predominantly fine-grained facies to a succession of conglomerates that occurred at ~30 Ma indicates progradation of a submarine fan. During the same time interval, sediment accumulation rates increased as a result of enhanced rates of crustal loading in the rear of the wedge (backthrusting along the Insubric Line (Giger 1991; Bernoulli et al. 1993; Schmid et al. 1996). This implies that fan progradation was caused by an increase in supply rates of sediment (see above and conceptual models of Heller and Paola 1992). Also at 30 Ma, the Molasse develops from an underfilled (Flysch deposits) to an overfilled basin (Molasse deposits) as a result of an increase in sediment flux (Figs. 4B, 8; Sinclair 1997). In the north, the presence of a terrestrial facies that lasted until the Aquitanian/Burdigalian boundary suggests that the phase of enhanced supply rates of sediment continued until ~20 Ma (see also Fig. 7); however, since the basin started to be underfilled at that time, supply rates of sediment had to decrease approximately 1–2 m.y. prior to 20 Ma (see also Schlunegger et al. 1997a). Similarly, the presence of massive coarse-grained conglomerates in the south that were deposited at a rate of ~250 m/m.y. between 30 and 24/22 Ma (Bernoulli et al. 1993) are interpreted to reflect enhanced flux of sediment during this time interval. Also in the south, approximately 2 m.y. prior to 20 Ma, the facies start to fine upward, indicating retreat of the submarine depositional systems. Because average accumulation rates of sediment also decreased to <150 m/m.y. during the same time interval (Bernoulli et al. 1993), the retreat of depositional systems suggests a decrease in supply rates of sediment (Fig. 8; e.g. Heller and Paola 1992).

In the south, between ~18 and 16 Ma, deposition of sandstones and conglomerates occurred at a rate of ~500 m/m.y. This coarse-grained facies is overlain by sandstone/mudstone alternations that were deposited at presumably lower sediment accumulation rates (Fig. 8; Bernoulli et al. 1993). The short-term increase in sediment accumulation rates and the presence of a coarse-grained facies as recorded by the Lucino Conglomerate might reflect initiation of the Lombardic phase of deformation (Schumacher et al. 1997). This interpretation is supported by the petrographic composition of conglomerates that reveal a shift in the clast suite towards predominance of detritus derived from the Southern Alpine nappes (Giger 1991). Despite ongoing thrust front propagation in the Southern Alpine nappes after 18 Ma (Fig. 3B; Schmid et al. 1996), the facies fined upward. This implies that supply rates of sediment were presumably low after deposition

of the Lucino Conglomerate. Because sediment flux was reduced prior to and after deposition of the Lucino Conglomerate, the present author interprets that, except for the Lucino-Conglomerate time, the Lombardic phase of deformation did not disturb the general decrease in average supply rate of sediment to the basin (Fig. 8). In the north, the regression at ~16.5 Ma was interpreted as the result of a ~50% increase of supply rates of sediment caused by enhanced exhumation of the Aar massif (Matter 1964; Fig. 11 C in Schlunegger et al. 1997d). This implies that after deposition of the OMM, average supply rates of sediment were <75% of the pre-20-Ma sediment flux (Fig. 8).

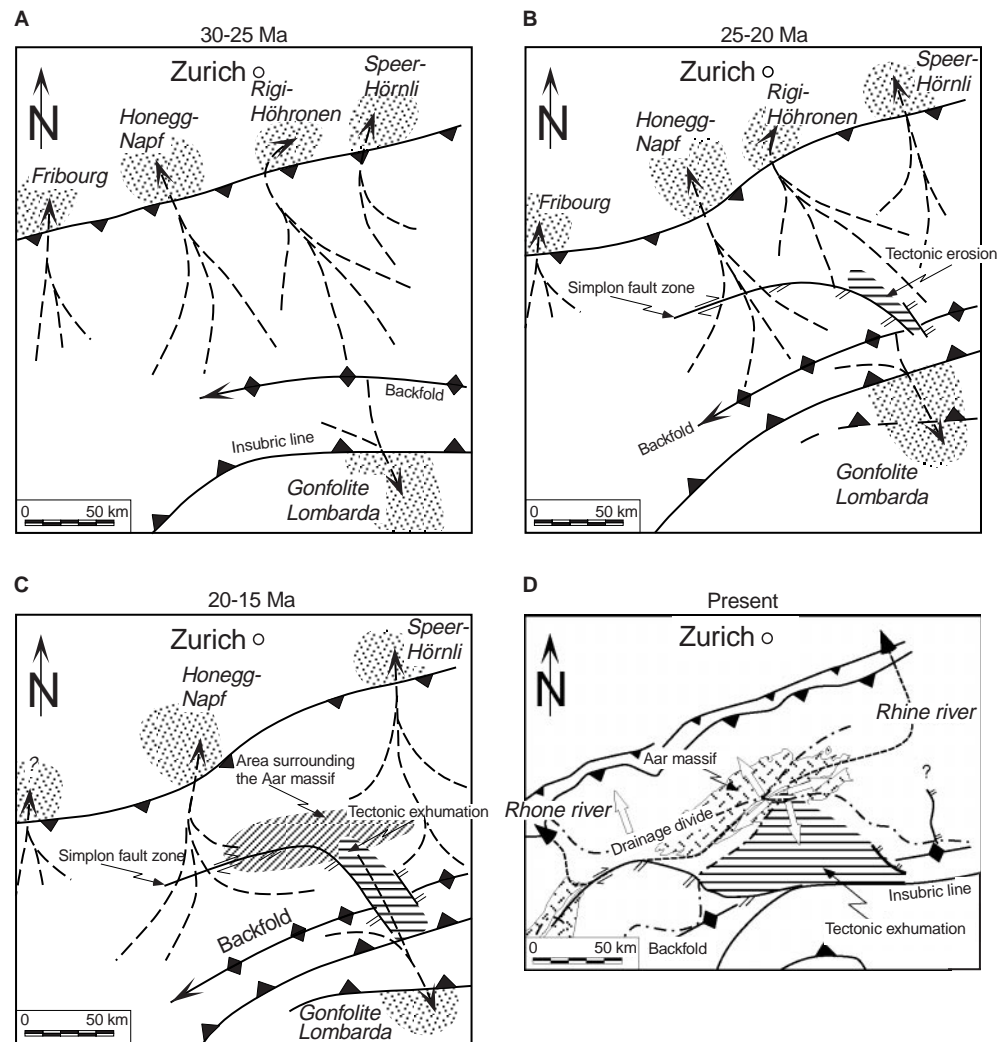
Network of the Alpine drainage basin and erosion rates

Knowledge about temporal shifts of average supply rates of sediment and the size of the drainage basin allows estimates of temporal variations of erosion rates which equals sediment yields or fluxes. Herein the evolution of the exhumation pattern and the drainage network of the Alps that was reconstructed by Schlunegger et al. (1998) and Schlunegger and Willett (in press) is discussed combining the information from sedimentary petrography of the conglomerates, the cooling history of present-day exposed rocks and the structural evolution of the Swiss Alps.

According to Mancktelow (1992), Mancktelow and Grasemann (1993), Schlunegger et al. (1998) and Schlunegger and Willett (in press), tectonic exhumation and surface erosion resulted in a decrease in the total exhumation from 25 km in the rear of the wedge to ca. 10 km in the external massifs. Tectonic exhumation accomplished by slip along the Simplon Fault Zone in the west (Mancktelow 1992; Steck and Hunziker 1994) and the Forcola normal fault in the east (Schmid et al. 1996) exposed the crystalline core of the Lepontine Dome (Fig. 2A), and caused an approximately 50-km-northward shift in the drainage divide from the area of the backfold in the rear of the wedge (Fig. 9A, B) to the region of the Aar massif (Fig. 9C, 9D; Schlunegger et al. 1998). In the Lepontine Dome, tectonic exhumation resulted in maximum erosion rates of ~5 km/m.y. around 20 Ma according to thermal models of cooling and erosion (Grasemann and Mancktelow 1993; Schlunegger and Willett, in press).

Besides tectonic exhumation, fluvial processes modified the topography of the evolving Alps. Three phases of drainage basin evolution occurred in the central Swiss Alps between 30 Ma and the present (Schlunegger et al. 1998). During the first stage, prior to 20 Ma, transverse drainage systems were present north and south of the main drainage divide that was formed by the backfold in the rear of the wedge (Figs. 9A, B). The distance between the northern and southern tip of the wedge and the main drainage divide measured ~140 and ~40 km, respectively.

Fig. 9 Evolution of the Alpine drainage network during the time intervals between **A** 30 and 5 Ma, **B** 25 and 20 Ma, and **C** 20 and 15 Ma. This reconstruction is based on the combined information about the petrographic evolution of the foreland basins and the structural evolution of the Alps. **D** The present-day Alpine drainage network and the general drainage direction of the Aare/Reuss rivers, the Rhine River, the Rhone River and the Ticino River. Note that the drainage network evolves from an across-strike to an orogen-parallel drainage direction. (Modified after Schlunegger et al. 1998)



During the second stage of drainage basin evolution, between ~ 20 – 15 Ma, the courses of the north Alpine palaeorivers were deflected around the hinge of the growing Aar massif (Fig. 9C), and the predominantly north/south-oriented drainage pattern north of the main drainage divide changed to the present-day orogen-parallel dispersion (Rhine and Rhone rivers; Fig. 9D). Furthermore, as outlined herein, orogen-parallel oriented slip along the Simplicon Fault Zone resulted in a 50-km northward shift of the main Alpine drainage divide to the area surrounding the Lepontine Dome (Fig. 9D). Finally, at ~ 18 Ma, the predominance of South Alpine clasts in the Gonfolite Lombardia indicates that the area of enhanced exhumation of the southern Alpine palaeorivers shifted southward (Fig. 9C). Despite the significant modification in the configuration of the drainage basins after 20 Ma, the sum of the size of the Alpine drainage basins remained nearly constant (Fig. 9C).

At 15 Ma, the present-day Alpine drainage network (Fig. 9D) was already established. The last stage of

drainage basin evolution, between 15 Ma and the present, is characterized by further downcutting of the Alps (Schlunegger et al. 1998).

Because the total size of the Alpine drainage basin remained nearly constant between 30 Ma and the present (see above), temporal shifts in the sum of supply rates of sediment to the North and to the South (Fig. 8) are interpreted in terms of temporal changes of average erosion rates. As outlined herein, average supply rates of sediment to the adjacent foreland basins were enhanced between 30 and 22/20 Ma, implying high Alpine erosion rates during that time interval. 2 millions of years prior to 20 Ma, average supply rates of sediment to both the North and the South Alpine Foreland Basin started to decrease, suggesting initiation of a phase of reduced Alpine erosion rates. It appears that enhanced exhumation of the Southern Alpine nappes between ~ 18 and 16 Ma, and the increase in exhumation of the Aar massif after 16 Ma, did not disturb the overall reduction in Alpine erosion rates (see discussion above).

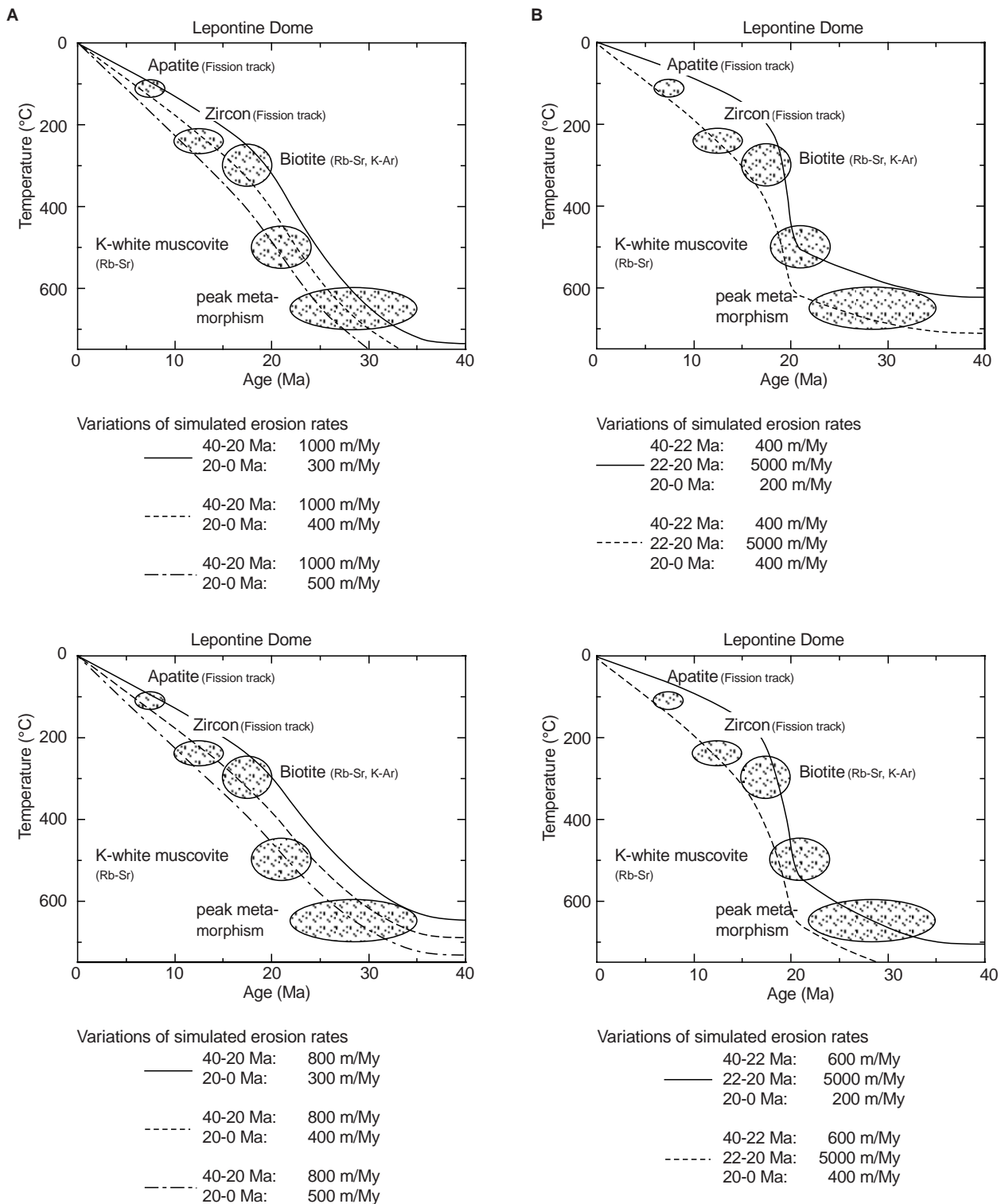


Fig. 10A, B Erosion rates of the Lepontine Dome that were determined using a numerical model of cooling and erosion. **A** The model was run for high rates of surface erosion between 40 and 20 Ma, followed by a period with significantly lower rates of surface erosion. **B** The cooling path of the present-day exposed rocks of the Lepontine Dome can also be simulated assuming a

short period of very rapid tectonic exhumation. In both cases surface erosion rates are significantly higher between 40 and 20 Ma than after 20 Ma. See Schlunegger and Willett (in press) for complete presentation and discussion of the model parameters. (Modified after Schlunegger and Willett, in press)

Thermo-chronological evolution of the drainage basin

Schlunegger and Willett (in press) tested the hypothesis of a decrease in average Alpine erosion rates for the area of the Lepontine Dome using thermal models of cooling and erosion. These authors calculated average erosion rates for the Lepontine Dome based on one-dimensional simulations of the cooling history of this area (Fig. 10). They simulated the case of surface erosion using constant erosion rates over long periods of time (Fig. 10A), and the scenario of tectonic exhumation with a short period of extremely high erosion rates (Fig. 10B). For the case of surface erosion, the cooling ages were best fit by early, high erosion rates of $\sim 800\text{--}1000\text{ m/m.y.}$ prior to 20 Ma, followed by a period with significantly lower erosion rates of $300\text{--}500\text{ m/m.y.}$ Tectonic exhumation was modelled applying an erosion rate of 5000 m/m.y. over a 2-m.y. period from 22 to 20 Ma, thereby simulating the rapid removal of a 10-km-thick upper plate (Steck and Hunziker 1994). The results of this model run (Fig. 10B) suggest that even with the tectonic exhumation, erosion rates were significantly higher prior to 22 Ma ($400\text{--}600\text{ m/m.y.}$) than after 20 Ma ($200\text{--}400\text{ m/m.y.}$).

Discussion

Implications for the evolution of the Alpine drainage pattern

The evolution of the drainage pattern as presented in Fig. 9 is a function of the ratio between the rates of crustal uplift and those of surface erosion. If erosion rates are higher than crustal uplift rates, a transverse drainage network develops (Burbank et al. 1996). In this case, the location of enhanced rates of surface erosion tends to shift towards the rear of the wedge that forms the major drainage divide (Willett et al. 1993; Koons 1994; Anderson 1994) irrespective of the pattern of strain release in the subsurface (Koons 1994). This is the case because the time intervals that are required for fluvial systems to reach steady state is much shorter ($<100\text{ k.y.}$; Allen 1997) than those for lithospheric processes (several million years; e.g. Jordan et al. 1993; Schmid et al. 1996). Alternatively, if surface erosion rates are lower than crustal uplift rates, a surface uplift results which may cause deflection in the courses of the palaeorivers around the hinges of growing structures. The resulting drainage pattern reveals both along- and across-strike orientations of palaeorivers (Tucker and Slingerland 1996; Burbank et al. 1997).

According to these theoretical models, the present author believes that prior to 20 Ma, erosion rates were higher than or equalled rates of crustal uplift. Indeed, erosion rates in the Alps were enhanced during the time interval between 40 and 20 Ma as indicated by

stratigraphic data from the foreland basins (Fig. 7; Sinclair 1997) and by thermo-chronological information from the drainage basin (Fig. 10). After 20 Ma, however, average crustal uplift rates were presumably higher than erosion rates as indicated by the deviation in the courses of the Alpine rivers around growing structures (e.g. the Aar massif).

Implications for Alpine tectonics

Based on coupled erosion-mechanical models for the evolution of orogens on a crustal scale, Willett et al. (1993) concluded that the large-scale evolution of orogenic wedges is controlled by the vergence of subduction and erosion rates (Fig. 11). If no erosion occurs on the surface of the orogen, then the evolving wedge adapts a

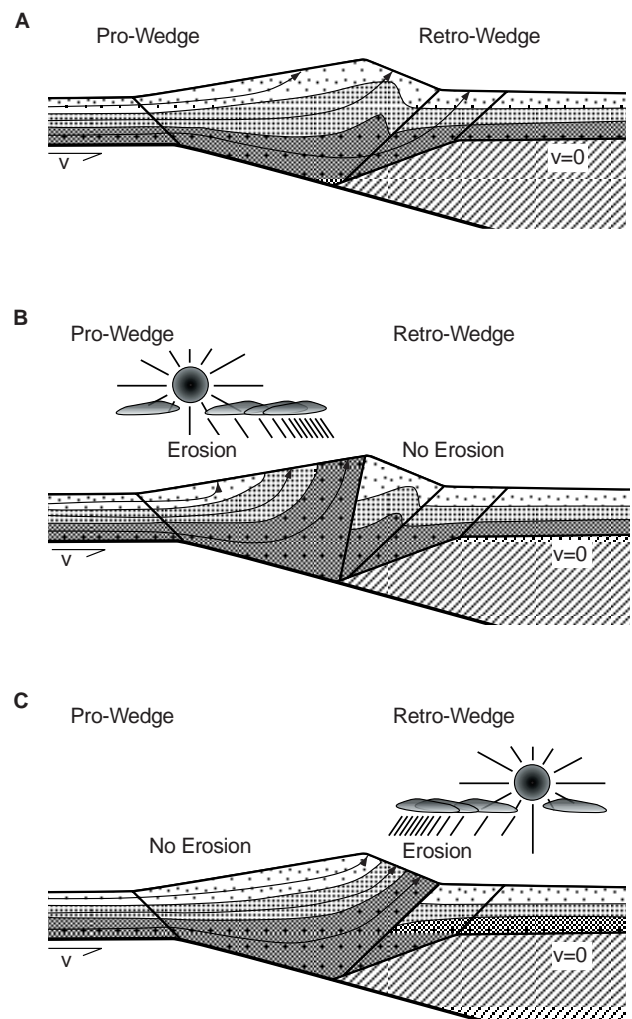
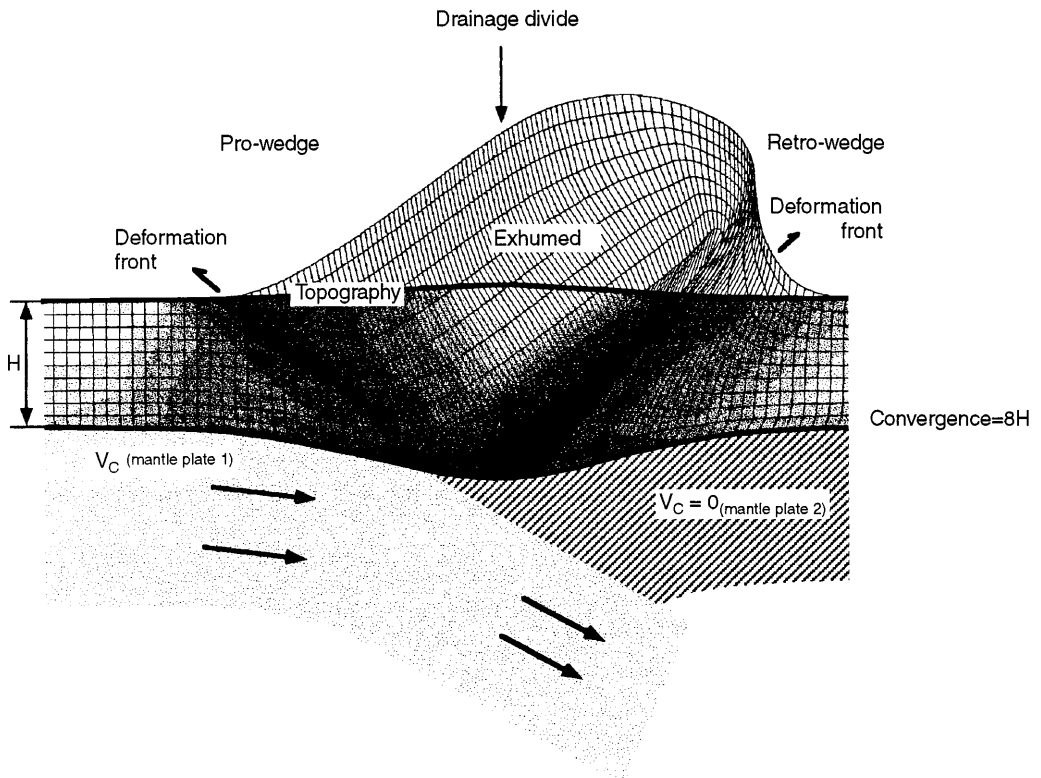
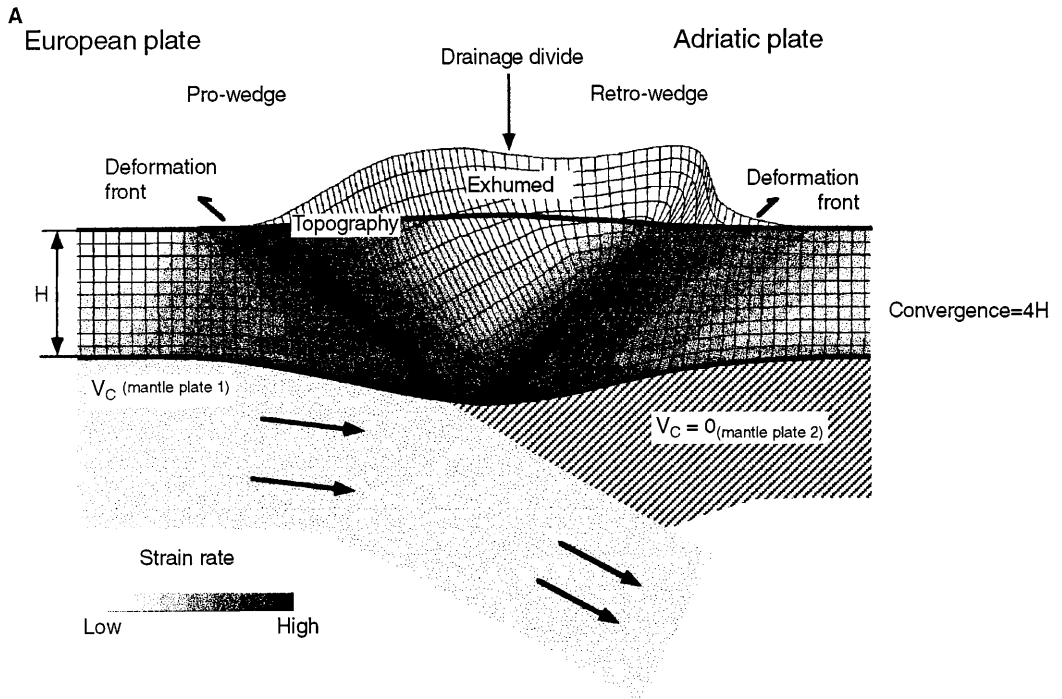


Fig. 11A–C Conceptual model, showing the evolution of an orogenic wedge as a function of the vergence of subduction and the location of enhanced surface erosion. Note that the velocity field and the exhumation path of the lithosphere is a function of the precipitation pattern. **A** Orogen with no erosion, **B** orogen with enhanced erosion on the pro-wedge side and **C** orogen with enhanced erosion on the retro-wedge side. (Modified after Willett et al. 1993)



H :	relative thickness of the crust
Convergence	Total relative convergence between two plates, related to the thickness of the crust
V_C	Relative convergence velocity, related to the thickness of the crust

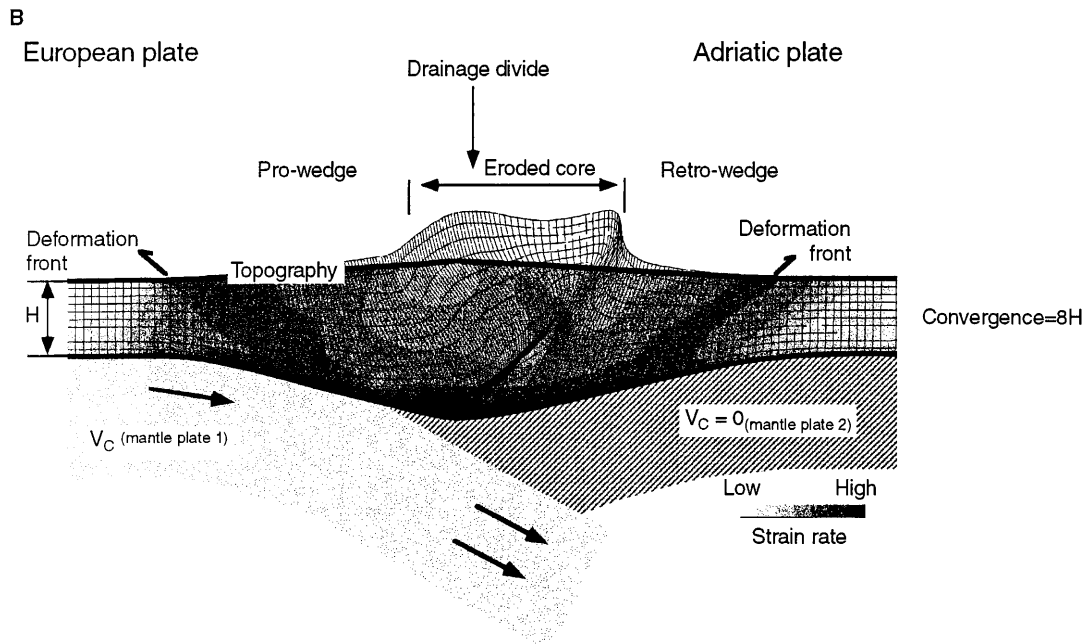


Fig. 12 **A** Modelled deformation and exhumation of the orogen after convergence of $4 \times H$ and $8 \times H$ (H is the relative thickness of the modeled crust, i.e. 25 km for the Alpine case). Eroded mass is shown by unfilled mesh above the ground surface. See text for further explanation, and Willett et al. (1993) and Schlunegger and Willett (in press) for discussion and presentation of the model parameters. (Modified after Schlunegger and Willett, in press). **B** Modelled deformation and exhumation for an orogen that experienced a significant decrease in average erosion rates after convergence of $4H$. See Schlunegger and Willett (in press) for presentation and justification of the model parameters, and text for further discussion. (Modified after Schlunegger and Willett in press)

distinct geometry with a low-tapered pro-wedge side facing the subducting plate, and a high-tapered retro-wedge side (Fig. 11A). Erosional processes lead to large-scale removal of mass from the wedge and cause the lithospheric velocity field to adjust to replace eroded material with material from within. As a result, areas that experience high rates of surface erosion have enhanced exhumation rates. Enhanced erosion on the pro-wedge side, for instance, results in formation of a non-deforming retro-wedge against which pro-wedge material is decoupled and exhumed (Fig. 11B). In contrast, steady-state retro-wedge erosion results in high rates of crustal deformation and the formation of a step-up shear zone on the retro-side of the wedge (e.g. the Insubric Line; Fig. 11C).

Giger (1991) and Schlunegger et al. (1993, 1998) suggested that prior to 20 Ma the main Alpine drainage divide was formed by backfolding (Figs. 2A, 9A, 9B) mechanically linked to backthrusting along the Insubric Line (Schmid et al. 1996). According to coupled erosion-mechanical models as outlined herein, the formation of a drainage divide in this part of the Alps was controlled by the vergence of subduction (see also

Beaumont et al. 1996; Schlunegger and Willett, in press).

Prior to 20 Ma, the high ratio between the rates of surface erosion and those of crustal uplift resulted in a shift in the area of enhanced erosional exhumation towards the backfold (see above). This interpretation is supported by the clast suite of conglomerates from the NABF that indicate a continuous increase in detritus derived from the rear of the wedge (Schlunegger et al. 1998). This implies that although lithospheric processes controlled initial formation of a drainage divide in the area of the backfold (e.g. Fig. 11A), surface processes were likely to have enhanced the rates of crustal thickening in the rear of the wedge in order to keep the wedge in a steady state (e.g. Fig. 11C). Alternatively, Sinclair (1997) suggested that enhanced rates of surface erosion in the rear of the wedge were controlled by an elastic rebound of the Alps surrounding the Insubric Line due to slab break-off (Davis and von Blanckenburg 1995). Numerical models by Beaumont et al. (1996) suggest that isostatic compensation of the crust after underplating of crustal material beneath the Adriatic plate might also have resulted in enhanced rates of surface uplift in the rear of the wedge and in enhanced rates of surface erosion. At around 20 Ma, however, average rates of surface erosion and presumably tectonic exhumation (Fig. 10B) started to decrease. At the same time, the ratio between the rates of crustal uplift and surface erosion increased as indicated by the deflection of the courses of the north Alpine palaeorivers around the hinges of growing structures (e.g. the Aar massif; Fig. 9C). This implies that the rates at which mass was added onto the wedge by lithospheric processes started to exceed the rates of erosion, causing the Alpine orogenic wedge to become supercritical. As a result, the wedge had to lower its

taper by accretion of material into the toe of the orogen (Davis et al. 1983; DeCelles and Mitra 1995). It appears, therefore, that the significant reduction in average erosion rates at 20 Ma is likely to have controlled initiation of propagation of the Alpine tip into the Southern Alpine nappes at ~18 Ma and into the Jura Mountains between 20 and 15 Ma (Schmid et al. 1996). In this case, expansion of the tip of the orogenic wedge towards the distal forelands was the structural response of the Alps to the change in the erosional processes in order to stay at an at-yield mechanical state. Alternatively, ongoing indentation between the converging plates might have enhanced the rates of crustal accretion and initiated a phase of orogenic growth. In this case, the reconstructed rates of plate convergence during the Oligocene and Miocene that are based on preserved volumes of upper crust should have increased. This was, however, not the situation for the Alps (Schmid et al. 1996).

Schlunegger and Willett (in press) tested the significance of the reduction in average erosion rates on the structural evolution of a Coulomb wedge (Fig. 1) using a two-dimensional, coupled erosion-mechanical model. They related the relative convergence velocity between the two plates V_c to the thickness H of the deformable crust which measures ~25 km (upper crust; Fig. 3). During the first model run, erosion rates were kept constant. Convergence of $8 \times H$ (i.e. 200 km) at constant erosion rates of ~1 km/m.y. resulted in the formation of an orogen with an asymmetrical surface pattern of exhumation (Fig. 12A) in response to the polarity of subduction (see also Fig. 11). Exhumation of material exposed at the surface of the modelled orogen (Fig. 12A) increases progressively from the tip to the rear of the wedge. This is approximately the pattern observed in the Alps prior to 20 Ma (Fig. 3). However, because the model has reached a mass-flux steady state between the rates of mass into and out of the orogen, continued convergence appears to lead to enhanced exhumation but not to outward growth of the orogen. During the second model run, presented in Fig. 12B, erosion rates were equivalent to those in the model of Fig. 12A. However, after convergence of $4 \times H$ (i.e. 100 km), erosion rates were reduced by a factor of 8 resulting in an average erosion rate of $0.025 V_c$ (i.e. 120 m/m.y.). This appears not to be sufficient to balance the convergent mass flux, and the orogen changes from a steady state (Fig. 12A) to a constructive state of growth during which the peripheral areas of the orogen are incorporated into the wedge by frontal accretion (Fig. 12B). This pattern of exhumation and deformation is consistent with the observations from the Alps in which a phase of rapid erosion of the Lepontine Dome was succeeded by a phase of outward growth of the Alps at low erosion rates (Figs. 3B, 10).

Conclusion

The synthesis of the available stratigraphic and structural data, coupled with published numerical models of erosion and lithospheric deformation, suggests that erosion rates had a great potential to have controlled the large-scale tectonic evolution of the Alps. Specifically, it appears that enhanced rates of backthrusting along the Insubric Line were controlled by high surface erosion rates prior to 20 Ma. The significant decrease in average erosion rates at ~20 Ma appears to have been instrumental in changing the crustal dynamics from a phase of enhanced exhumation in the rear of the Alps to a period of crustal growth at reduced exhumation rates.

Although the available information suggests that erosion rates were a significant parameter controlling the evolution of the Swiss Alps, a complete discussion of the complex interaction between surface erosion and strain partitioning in the Alps requires a three-dimensional numerical model that couples surface processes (fluvial erosion of bedrock and colluvium, hillslope processes, glacial erosion), climate (differential precipitation rates) and lithospheric processes. Such a theoretical model, however, is not yet available. Furthermore, since erosion rates are an important issue for the Alpine evolution, we also need data for palaeotemperature and palaeoprecipitation for the area surrounding the central Alps. Finally, more data have to be collected and synthesized from the South Alpine Foreland Basin to better constrain the temporal and spatial variations of average supply rates of sediment to the south.

Acknowledgements This work was supported by Friedrich Schiller University of Jena, Germany. Special thanks go to T. Jahr, T. Voigt, S. v.d. Klauw (FSU Jena) and S. Willett (University of Washington) for fruitful discussions, and to H. von Eynatten (FSU Jena) for a critical review of the manuscript. The excellent reviews by P. Allen and S. Schmid significantly improved the science and the quality of this paper.

References

- Allen PA (1997) Earth surface processes. Blackwell, Oxford
- Allen PA, Mange MA, Matter A, Homewood P (1985) Dynamic palaeogeography of the open Burdigalian seaway, Swiss Molasse basin. *Eclogae Geol Helv* 78:351–381
- Anderson RS (1994) Evolution of the Santa Cruz Mountains, California, through tectonic growth and geomorphic decay. *J Geophys Res* 99:20161–20180
- Batt GE, Braun J (1997) On the thermomechanical evolution of compressional orogens. *J Geophys Int* 128:364–382
- Beaumont C, Ellis S, Hamilton J, Fullsack P (1996) Mechanical model for subduction-collision of Alpine-type compressional orogen. *Geology* 24:675–678
- Berger JP (1996) Cartes paléogéographiques-palinspastiques du bassin molassique suisse (Oligocène inférieur–Miocène moyen). *N Jahrb Geol Paläontol Abh* 202:1–44

- Bernoulli D, Giger M, Müller DW, Ziegler URF (1993) Sr-isotope stratigraphy of the Gonfolite Lombarda Group ("South-Alpine Molasse", northern Italy) and radiometric constraints for its age of deposition. *Eclogae Geol Helv* 86:751–767
- Bertotti G, Picotti V, Cloetingh S (1998) Lithospheric weakening during "retroforeland" basin formation: tectonic evolution of the central South Alpine foredeep. *Tectonics* 17:131–142
- Burbank DW, Meigs A, Brozovic N (1996) Interactions of growing folds and coeval depositional systems. *Basin Res* 8:199–223
- Burkhard M (1988) L'Hélievétique de la bordure occidentale du massif de l'Aar (évolution tectonique et métamorphique). *Eclogae Geol Helv* 81:559–583
- Chapple WM (1978) Mechanics of thin-skinned fold-and-thrust belts. *Geol Soc Am Bull* 97:1189–1198
- Colombo F (1994) Normal and reverse unroofing sequences in syntectonic conglomerates as evidence of progressive basinward deformation. *Geology* 22:235–238
- Davis DM, Suppe J, Dahlen FA (1983) Mechanics of fold-and-thrust belts and accretionary wedges. *J Geophys Res* 88:1153–1172
- Davis JH, Blanckenburg F von (1995) Slab breakoff: a model of lithosphere detachment and its test in the magmatism and deformation of collisional orogens. *Earth Planet Sci Lett* 129:85–102
- DeCelles PG, Mitra G (1995) History of the Sevier orogenic wedge in terms of critical taper models, northeast Utah and southwest Wyoming. *Geol Soc Am Bull* 107:454–462
- Flemings PB, Jordan TE (1989) A synthetic stratigraphic model of foreland basin development. *J Geophys Res* 94:3851–3866
- Füchtbauer H (1959) Die Schüttungen im Chatt und Aquitan der deutschen Alpenvorlandmolasse. *Eclogae Geol Helv* 51:928–941
- Füchtbauer H (1964) Sedimentpetrographische Untersuchungen in der älteren Molasse nördlich der Alpen. *Eclogae Geol Helv* 61:157–298
- Gelati R, Napolitano A, Valdistrullo A (1988) La "Gonfolite Lombarda". Stratigrafia e significato nella evoluzione oligomiocena del margine sudalpino. *Riv Ital Paleontol Stratigr* 94:285–332
- Giger M (1991) Geochronologische und petrographische Studien an Geröllen und Sedimenten der Gonfolite Lombarda Gruppe (Südschweiz und Norditalien) und ihr Vergleich mit dem alpinen Hinterland. PhD thesis, Univ Bern, 227 pp
- Grasemann B, Mancktelow NS (1993) Two-dimensional thermal modelling of normal faulting: the Simplon fault zone, Central Alps, Switzerland. *Tectonophysics* 225:155–165
- Gunzenhauser BA (1985) Zur Sedimentologie und Paläogeographie der oligo-miocänen Gonfolite Lombarda zwischen Lago Maggiore und der Brianza. *Beitr Geol Karte Schweiz* 159:1–114
- Heller PL, Paola C (1992) The large-scale dynamics of grain-size variation in alluvial basins: Application to syntectonic conglomerate. *Basin Res* 4:91–102
- Homewood P, Allen PA, Williams GD (1986) Dynamics of the Molasse Basin of western Switzerland. *Int Assoc Sedimentol Spec Publ* 8:199–217
- Hunziker JC, Hurford AJ, Calmbach L (1997) Alpine cooling and uplift. In: Pfiffner OA, Lehner P, Heitzmann P, Müller S, Steck A (eds) Results of the National Research Program 20 (NRP 20). Birkhäuser, Basel, pp 260–264
- Jordan TE, Allmendinger RW, Damanti JF, Drake RE (1993) Chronology of motion in a complete thrust belt: the Precordillera, 30–31°S, Andes Mountains. *J Geol* 101:135–156
- Keller B (1989) Fazies und Stratigraphie der Oberen Meeresmolasse (Unteres Miozän) zwischen Napf und Bodensee. PhD thesis, Univ Bern, Bern, 277 pp
- Kempf O, Bolliger T, Kälin D, Engesser B, Matter A (1998) New magnetostratigraphic calibration of Early to Middle Miocene mammal biozones of the North Alpine foreland basin. In: Aguilar JP, Legendre S, Michaux J (eds) Actes du Congrès BiochronM'97. Mém Trav EPHE 21, Inst Montpellier, pp 547–561
- Koons PO (1994) Three-dimensional critical wedges: tectonics and topography in oblique collisional orogens. *J Geophys Res* 99:12301–12315
- Mägert M (1998) Sedimentation und Entwicklung des Beichlen-Schuttfächers (Untere Süswassermolasse – Entlebuch). Thesis, Univ Bern, 125 pp
- Mancktelow NS (1992) Neogene lateral extension during convergence in the Central Alps: evidence from interrelated faulting and backfolding around the Simplon pass (Switzerland). *Tectonophysics* 215:295–317
- Mandl G (1988) Mechanics of tectonic faulting: models and basic concepts. Elsevier, Amsterdam
- Matter A (1964) Sedimentologische Untersuchungen im östlichen Napfgebiet (Entlebuch – Tal der Grossen Fontanne, Kt. Luzern). *Eclogae geol Helv* 57:315–384
- Matter A, Homewood P, Caron C, Rigassi D, Van Stuijvenberg J, Weidmann M, Winkler W (1980) Flysch and molasse of western and central Switzerland. In: Trümpy R (ed) *Geology of Switzerland, a guidebook. Part B, Excursions. Schweiz Geol Komm*, pp 261–293
- Maurer H, Funk HP, Nabholz W (1978) Sedimentpetrographische Untersuchungen an Molasse-Abfolgen der Bohrung Linden 1 und ihrer Umgebung (Kt. Bern). *Eclogae Geol Helv* 71:497–515
- Meigs AJ, Burbank DW (1997) Growth of the South Pyrenean orogenic wedge. *Tectonics* 16:239–258
- Mosar J (1988) Métamorphisme transporté dans les Préalpes. *Bull Suisse Minéral Pétrogr* 68:77–94
- Pfiffner OA, Heitzmann P (1997) Geologic interpretation of the seismic profiles of the Central Traverse (lines C1, C2, C3-north). In: Pfiffner OA, Lehner P, Heitzmann P, Müller S, Steck A (eds) Results of the National Research Program 20 (NRP 20). Birkhäuser, Basel, pp 115–122
- Pfiffner OA, Sahli S, Stäubli M (1997) Structure and evolution of the external basement uplifts. In: Pfiffner OA, Lehner P, Heitzmann P, Müller S, Steck A (eds) Results of the National Research Program 20 (NRP 20). Birkhäuser, Basel, pp 139–153
- Platt JP (1986) Dynamics of orogenic wedges and the uplift of high-pressure metamorphic rocks. *Geol Soc Am Bull* 97:1037–1053
- Schlanke S (1974) Geologie der subalpinen Molasse zwischen Biberbrugg/SZ, Hütten/ZH und Aegerisee/ZG, Schweiz. *Eclogae Geol Helv* 67:243–331
- Schlanke S, Hauber L, Büchi U (1978) Lithostratigraphie und Sedimentpetrographie der Molasse in den Bohrungen Tschugg-1 und Ruppoldsried-1 (Berner Seeland). *Eclogae Geol Helv* 71:409–425
- Schlunegger F (1997) Controls of erosional denudation on the stratigraphy of foreland basins and on strain partitioning in the orogen: the Alps and the Molasse Basin. *GAEA Heidelbergensis* 3:305–306
- Schlunegger F, Willett SD (in press) Spatial and temporal variations in exhumation of the central Swiss Alps and implications for exhumation mechanisms. In: Brandon MT, Willett SD (eds) Exhumation processes: normal faulting, ductile flow and erosion. *Geol Soc Lond Spec Publ*
- Schlunegger F, Matter A, Mange MA (1993) Alluvial fan sedimentation and structure of the southern Molasse Basin margin, Lake Thun area, Switzerland. *Eclogae Geol Helv* 86:717–750
- Schlunegger F, Burbank DW, Matter A, Engesser B, Mödden C (1996) Magnetostratigraphic calibration of the Oligocene to Middle Miocene (30–15 Ma) mammal biozones and depositional sequences of the Swiss Molasse Basin. *Eclogae Geol Helv* 89:753–788

- Schlunegger F, Matter A, Burbank DW, Klaper EM (1997a) Magnetostratigraphic constraints on relationships between evolution of the central Swiss Molasse Basin and Alpine orogenic events. *Bull Geol Soc Am* 109:225–241
- Schlunegger F, Matter A, Burbank DW, Leu W, Mange MA, Máttyás J (1997b) Sedimentary sequences, seismofacies and evolution of depositional systems of the Oligo/Miocene Lower Freshwater Molasse Group, Switzerland. *Basin Res* 9:1–26
- Schlunegger F, Jordan TE, Klaper EM (1997c) Controls of erosional denudation in the orogen on foreland basin evolution: the Oligocene central Swiss Molasse Basin as an example. *Tectonics* 16:823–840
- Schlunegger F, Leu W, Matter A (1997d) Sedimentary sequences, seismic facies, subsidence analysis, and evolution of the Burdigalian Upper Marine Molasse Group, Central Switzerland. *AAPG Bull* 81:1185–1207
- Schlunegger F, Slingerland R, Matter A (1998) Crustal thickening and crustal extension as controls on the evolution of the drainage network of the central Swiss Alps between 30 Ma and the present: constraints from the stratigraphy of the North Alpine Foreland Basin and the structural evolution of the Alps. *Basin Res* 10:197–212
- Schmid SM, Aebli HR, Heller F, Zingg (1989) The role of the Periadriatic Line in the tectonic evolution of the Alps. In: Covard M, Dietrich D, Park RG (eds) *Alpine tectonics*. *Geol Soc Lond Spec Publ* 45:153–171
- Schmid SM, Pfiffner OA, Froitzheim N, Schönborn G, Kissling E (1996) Geophysical–geological transect and tectonic evolution of the Swiss–Italian Alps. *Tectonics* 15:1036–1064
- Schmid SM, Pfiffner OA, Schreurs G (1997) Rifting and collision in the Penninic Zone of eastern Switzerland. In: Pfiffner OA, Lehner P, Heitzmann P, Müller S, Steck A (eds) *Results of the National Research Program 20 (NRP 20)*. Birkhäuser, Basel, pp 160–185
- Schumacher ME, Schönborn G, Bernoulli D, Laubscher HP (1997) Rifting and collision in the Southern Alps. In: Pfiffner OA, Lehner P, Heitzmann P, Müller S, Steck A (eds) *Results of the National Research Program 20(NRP 20)*. Birkhäuser, Basel, pp 186–204
- Sinclair HD (1997) Flysch to Molasse transition in peripheral foreland basins: the role of the passive margin versus slab breakoff. *Geology* 25:1123–1126
- Sinclair HD, Allen PA (1992) Vertical versus horizontal motions in the Alpine orogenic wedge: stratigraphic response in the foreland basin. *Basin Res* 4:215–232
- Sinclair HD, Coakley BJ, Allen PA, Watts AB (1991) Simulation of foreland basin stratigraphy using a diffusion model of mountain belt uplift and erosion: an example from the central Alps, Switzerland. *Tectonics* 10:599–620
- Schönborn G (1992) Alpine tectonics and kinematic models of the central Southern Alps. *Mem Sci Geol (Padova)* 44:229–393
- Steck A, Hunziker J (1994) The Tertiary structural and thermal evolution of the Central Alps: compressional and extensional structures in an orogenic belt. *Tectonophysics* 238:229–254
- Tucker GE, Slingerland R (1996) Predicting sediment flux from fold and thrust belts. *Basin Res* 8:329–349
- Turcotte DL, Schubert G (1982) *Geodynamics: application of continuum physics to geological problems*. Wiley, New York
- Vollmayr T, Wendt A (1987) Die Erdgasbohrung Entlebuch-1, ein Tiefenausschluss am Alpennordrand. *Bull Ver Schweiz Petrol Geol Ing* 53:67–79
- Willett SD, Beaumont C, Fullsack P (1993) Mechanical model for the tectonics of doubly vergent compressional orogens. *Geology* 21:371–374